(2)

NAVAL POSTGRADUATE SCHOOL
Monterey, California

THESIS

CORRELATION OF AVHRR IMAGERY WITH SUB-SURFACE FEATURES IN THE CALIFORNIA CURRENT

by

Jeffrey Scott Best

June 1989

Thesis Advisor: Steven R. Ramp

SECURITY CLASSIFICATION OF THIS PAGE

REPORT DOCUMENTATION PAGE

Form Approved OMB No. 0704-0188

1a. REPORT SECURITY CLASSIFICATION UNCLASSIFIED	1b. RESTRICTIVE MARKINGS
2a. SECURITY CLASSIFICATION AUTHORITY	3. DISTRIBUTION/AVAILABILITY OF REPORT Approved for public release; distribution is unlimited.
2b. DECLASSIFICATION/DOWNGRADING SCHEDULE	
4. PERFORMING ORGANIZATION REPORT NUMBER(S)	5. MONITORING ORGANIZATION REPORT NUMBER(S)
6a. NAME OF PERFORMING ORGANIZATION Naval Postgraduate School 6b. OFFICE SYMBOL (If applicable) 68	7a. NAME OF MONITORING ORGANIZATION Naval Postgraduate School
6c. ADDRESS (City, State, and ZIP Code) Monterey, CA 93943-5000	7b. ADDRESS (City, State, and ZIP Code) Monterey, CA 93943-5000
8a. NAME OF FUNDING/SPONSORING ORGANIZATION 8b. OFFICE SYMBOL (If applicable)	9 PROCUREMENT INSTRUMENT IDENTIFICATION NUMBER
8c. ADDRESS (City, State, and ZIP Code)	10 SOURCE OF FUNDING NUMBERS PROGRAM ELEMENT NO / PROJECT NO / TASK NO / WORK UNIT ACCESSION NO.

11 TITLE (Include Security Classification) CORRELATION OF AVHRR IMAGERY WITH SUB-SURFACE FEATURES IN THE CALIFORNIA CURRENT (UNCLASSIFIED)

12 PERSONAL AUTHOR(S) Best, Jeffrey, S.

13a TYPE OF REPORT	13b TIME COVERED	14. DATE OF REPORT (Year, Month, Day)	15 PAGE COUNT
Master's Thesis	FROM _____ TO _____	June 1989	67

16 SUPPLEMENTARY NOTATION The views expressed in this thesis are those of the author and do not reflect the official policy or position of the Dept. of Defense or U.S. Government

17 COSATI CODES			18 SUBJECT TERMS (Continue on reverse if necessary and identify by block number)
FIELD	GROUP	SUB-GROUP	AVHRR Imagery, In-situ temperature field, Surface dynamic height field

19 ABSTRACT (Continue on reverse if necessary and identify by block number)

SST fields derived from AVHRR imagery are compared with subsurface temperature and surface dynamic height fields. The in-situ data collection was part of the Coastal Transition Zone (CTZ) cold filament experiments of 1987 and 1988. The results of the 1987 cruise show a subsurface maximum in the correlation coefficient between AVHRR SST and in-situ temperature at depth for all three phases of the cruise which is attributed to the temporal offset between the satellite image and the data collection. The results of the 1988 cruise show maximum correlations at the surface with significant correlations at the 95% level of confidence to about 130 - 150 m depth, with positive correlations to 310 - 350 m depth. Comparing the results of the 1987 and 1988 cruises shows that the offshore filament was much stronger both horizontally and vertically for the latter cruise.

20 DISTRIBUTION/AVAILABILITY OF ABSTRACT	21 ABSTRACT SECURITY CLASSIFICATION
☒ UNCLASSIFIED/UNLIMITED ☐ SAME AS RPT ☐ DTIC USERS	Unclassified
22a NAME OF RESPONSIBLE INDIVIDUAL Steven R. Ramp	22b TELEPHONE (Include Area Code) 408 646-3162
22c OFFICE SYMBOL 68Rc	

DD Form 1473, JUN 86 Previous editions are obsolete SECURITY CLASSIFICATION OF THIS PAGE

S/N 0102-LF-014-6603

Approved for public release; distribution is unlimited.

Correlation of AVHRR Imagery with Sub-Surface
Features in the California Current

by

Jeffrey S. Best
Lieutenant, United States Navy
B.S., United States Naval Academy

Submitted in partial fulfillment
of the requirements for the degree of

MASTER OF SCIENCE IN METEOROLOGY AND PHYSICAL OCEANOGRAPHY

from the

NAVAL POSTGRADUATE SCHOOL
1989

Author: _____
Jeffrey S. Best

Approved by: _____
Steven R. Ramp, Thesis Advisor

_____
Edward B. Thornton, Second Reader

_____
Curtis A. Collins, Chairman
Department of Oceanography

_____
Gordon E. Schacher,
Dean of Science and Engineering

ABSTRACT

SST fields derived from AVHRR imagery are compared with subsurface temperature and surface dynamic height fields. The *in-situ* data collection was part of the Coastal Transition Zone (CTZ) cold filament experiments of 1987 and 1988. The results of the 1987 cruise show a subsurface maximum in the correlation coefficient between AVHRR SST and *in-situ* temperature at depth for all three phases of the cruise which is attributed to the temporal offset between the satellite image and the data collection. The results of the 1988 cruise show maximum correlations at the surface with significant correlations at the 95% level of confidence to about 130 - 150 m depth, with positive correlations to 310 - 350 m depth. Comparing the results of the 1987 and 1988 cruises shows that the offshore filament was much stronger both horizontally and vertically for the latter cruise.

TABLE OF CONTENTS

LIST OF FIGURES

I. INTRODUCTION

Cold filaments off the California coast were first noticed in the spaceborne thermal and color imagery from the GOES and polar orbiting satellites (Bernstein et al., 1977; Ikeda and Emery, 1984; Kelly, 1985). A question arose immediately as to the depth penetration of these features and the representativeness of the surface fields of the underlying structure and dynamics. Some *in-situ* measurements in cold filaments were made as part of the Coastal Oceans Dynamic Experiment (CODE) (Kosro and Huyer, 1986; Flament et al., 1985) and Ocean Prediction Through Observation, Modeling, and Analysis (OPTOMA) (Mooers and Robinson, 1984; Reinecker et al., 1985, 1987) programs, which showed the need for a study more focussed on the cold filament problem.

The Coastal Transition Zone (CTZ) program was conceived to focus on the properties of cold filaments off the California coast, including their dynamics and biological ramifications (Brink and Hartwig, 1986; The CTZ Group, 1988). A stated goal of this program was to determine the representativeness of the surface imagery, including its ability to predict the subsurface thermal structure and dynamic height fields. Previous studies of vertical correlation in the California Current System using other data sets (Reinecker et al., 1985; Kosro and Huyer, 1986; Simpson et al., 1986; Reinecker et al., 1987) have shown mixed results: Some showed very high correlation between the surface or near surface fields and the subsurface fields, and others did not. These results are considered in greater detail in the discussion section.

The purpose of this thesis is to determine how well the subsurface temperature and dynamic height fields were represented by the satellite derived SST fields off Central California during the CTZ program of 1987 and 1988. These studies focussed entirely on the cold filaments and thus contain a greater number of data points in the filaments than were obtained during earlier studies.

The correlation between *in-situ* environmental parameters and AVHRR satellite imagery has not been thoroughly researched particularly in the complicated California Current System. The purpose of this study is to create a quasi-synoptic 3-dimensional

map of the hydrographic structure in various features off Point Arena and then correlate this data with the satellite Advanced Very High Resolution Radiometer (AVHRR) imagery for the corresponding time period.

The data collected was part of the Office of Naval Research (ONR) Coastal Transition Zone experiment from June 15 - 28, 1987 and from July 06 - 18 1988. It encompassed the region from just north of Pt. Arena, California (39° 15.0' N) south to about (37° 40.0' N) and from the coast to approximately 120 nm offshore. This area was chosen because of a strong cold filament that had been detected on the NOAA-9 AVHRR imagery for June 11, 1987. Another even stronger filament existed from just north of Pt. Arena to nearly 300 nm offshore for the July 1988 cruise. The source waters for these features appeared in the imagery to be from just north of Pt Arena.

The satellite imagery used was from the Advanced Very High Resolution (AVHRR) sensor aboard the NOAA-9 and NOAA-10 satellites. The imagery for both periods was cloud free in the area of interest and was excellent for locating the various features in both coastal and offshore regions. The primary images used in this study for the first cruise were June 16, June 21, and June 27, 1987 as these were the central dates for the three hydrographic surveys carried out during the cruise. The central images for the 1988 cruise were July 9th and 16th, the midpoints of the two sampling periods.

II. DATA AND METHODS

The *in-situ* data were collected as part of the Coastal Transition Zone Experiment pilot study (CTZE87) from the middle to the end of June 1987 and the main field experiment (CTZE88) from the 5th to the 19th of July 1988. The first cruise was divided into three phases: Phase I (CTD stations 1 - 54) ended when the first filament could no longer be followed non-ambiguously; Phase II (CTD stations 55 - 78) was ended by inclement weather; and Phase III (CTD stations 79 - 115) ended when the available cruise time expired. During the second (1988) cruise, a set grid pattern of 63 stations was sampled twice.

The station locations for the 1987 cruise were picked to best follow a strong cold filament originating just north of Pt. Arena (Figure 1). The first phase of the (CTZE87) cruise covered the entire experiment area with five transections of the filament ending with stations 47 through 54 along 125° 30' W (Figure 2). The second phase of the cruise began with station 55 on the 20th of June and concentrated on the area close to the coast where the source of the filament was believed to have originated (Figure 3). The third phase of the cruise began well offshore approximately 200 nm south west of Pt. Arena and made four transections of the deep, offshore filament extending well offshore (Figure 4). Several of the phase two stations were repeated.

The 1988 (CTZE88) cruise was divided into two parts with the first half covering 6 to 12 July and the second half 13 through 18 July. The grid area consisted of 63 stations extending from Pt. Arena to approximately 200 nm offshore with 15 nm spacing in the alongshore direction and 20 nm spacing in the across-shore direction (Figure 3).

Figure 1 AVHRR Imagery from June 16, 1987 with station locations for the CTZF 1987 cruise.

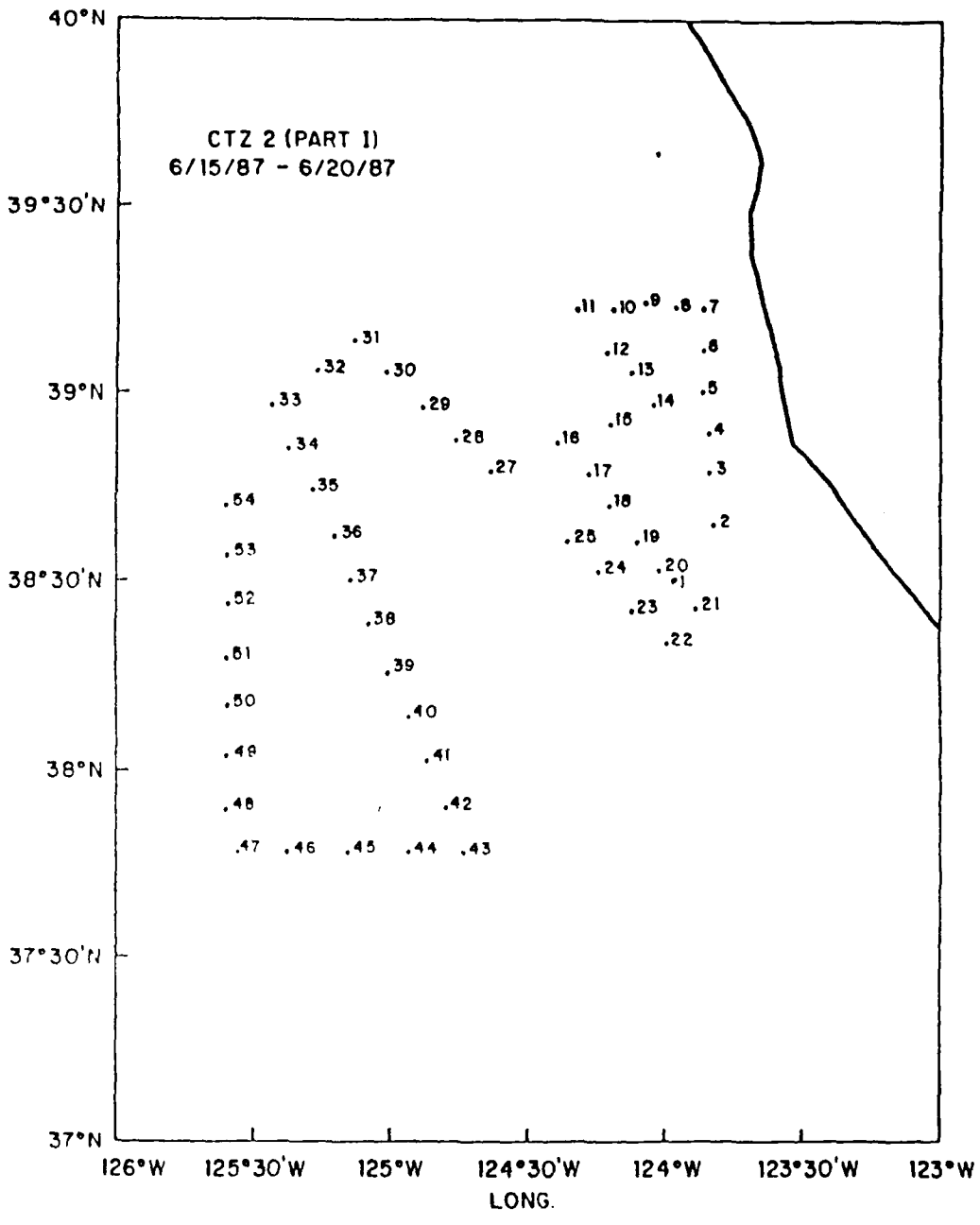

Figure 2 (a) CTD station numbers and locations for Phase I of the CTZE 1987 cruise.

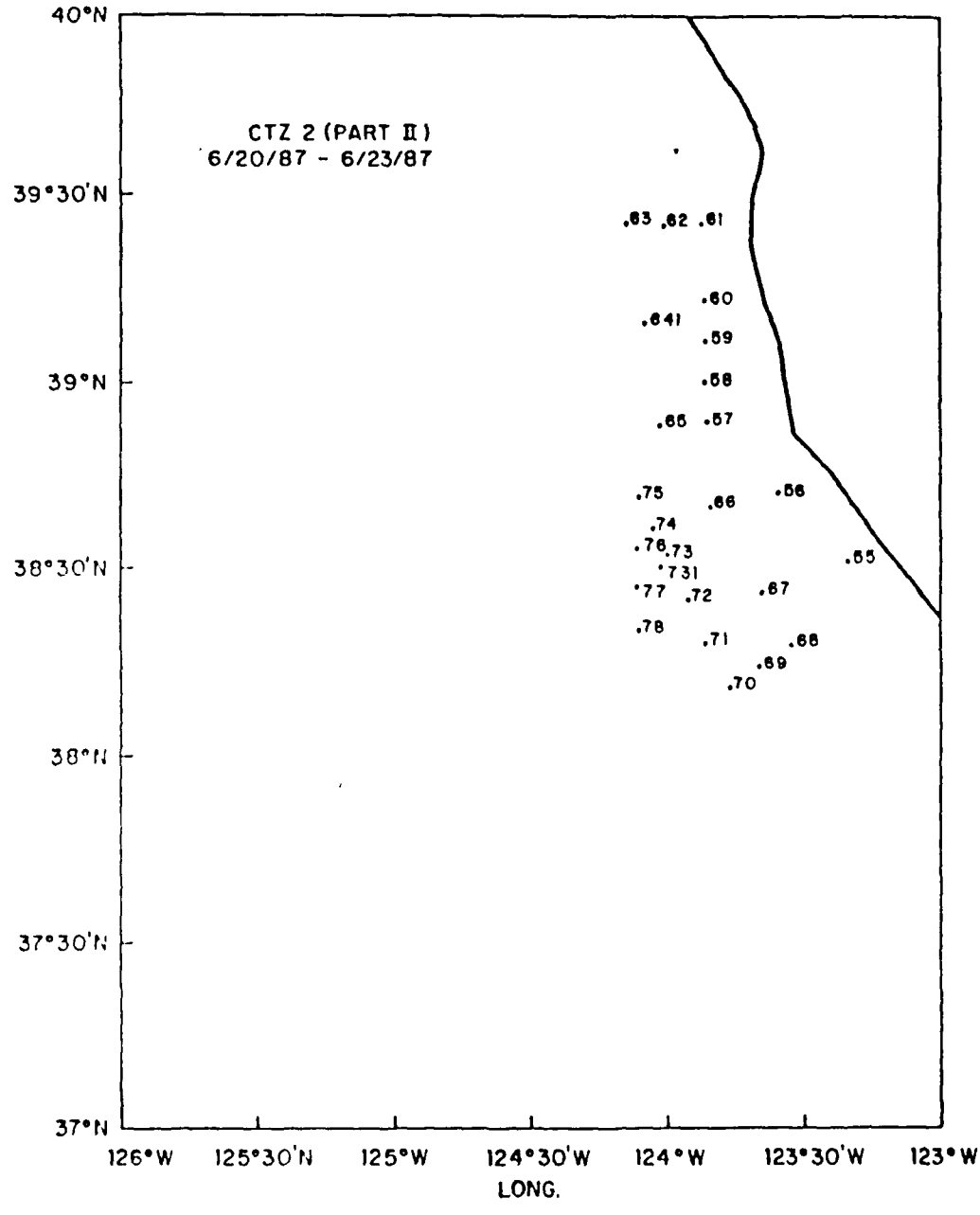

Figure 2 (b) CTD station numbers and locations for Phase II of the CTZE 1987 cruise.

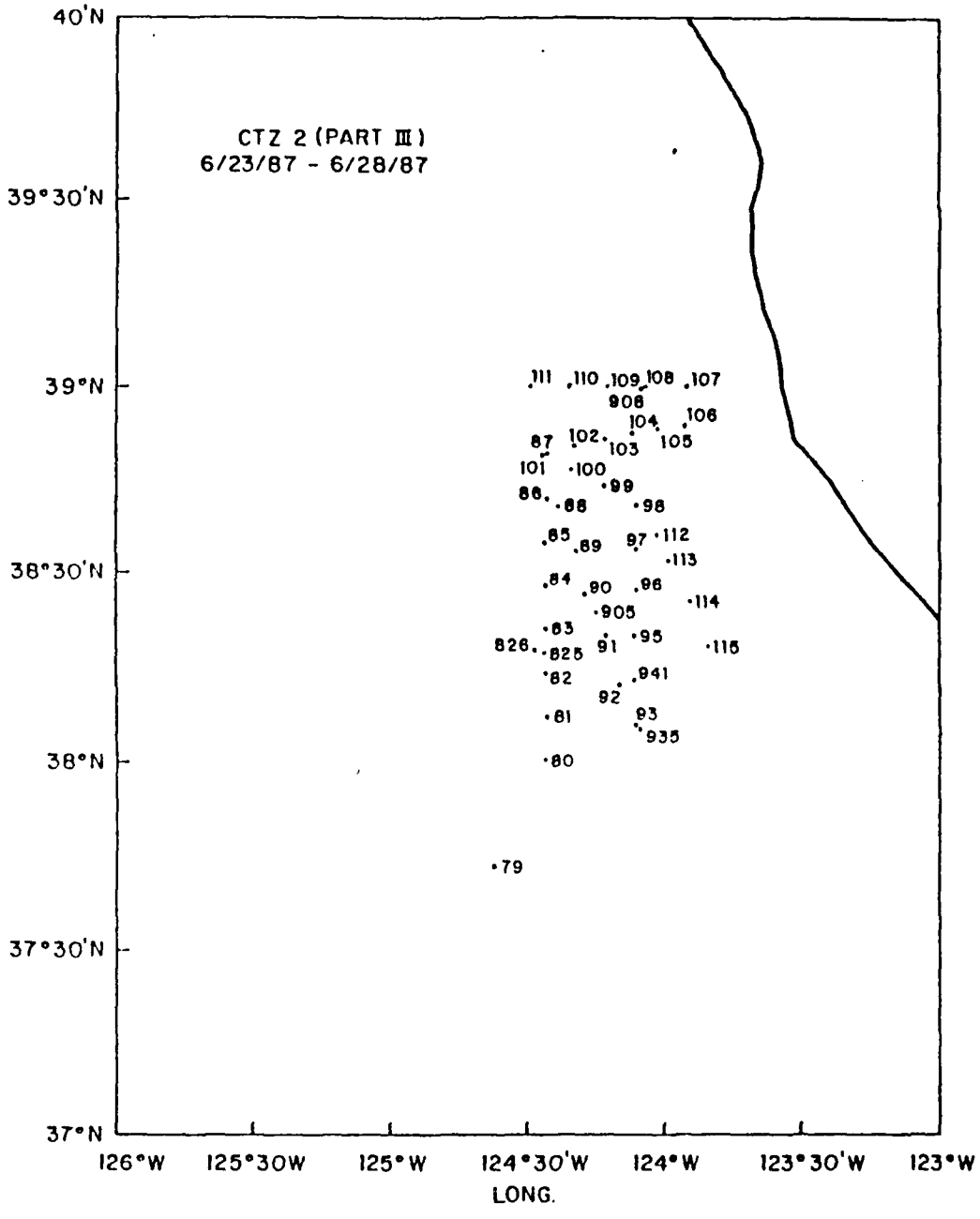

Figure 2 (c) CTD station numbers and locations for Phase III of the CTZE 1987 cruise.

Figure 3 AVHRR imagery for July 16, 1988 with CTZE88 station numbers and locations.

A. IN-SITU DATA ACQUISITION

The hydrographic data were acquired using a Neil Brown Mark III-B CTD. A General Oceanics rosette sampler was attached to the CTD and was equipped with twelve five liter Nisken bottles for *in-situ* water sampling. The data were acquired using an HP200 computer and stored on 3.5 inch diskettes. The data were then transferred to 9 track tape and processed on an IBM 3033 mainframe computer.

In addition to the CTD data, an underway data acquisition loop recorded 30 second averages of sea surface temperature and salinity, sea surface skin temperature, wind speed and direction, air temperature, dew point temperature, and visible and infrared radiation. The sensors used to acquire this data included Seabird temperature and conductivity sensors for the sea surface temperature and salinity, a Rosemount 100 ohm platinum resistance thermistor for the sea surface skin temperature, an R. M. Young anemometer for the wind speed and direction, a General Eastern dewpoint sensor for the air and dewpoint temperatures, and Epply pyronometers for the visible and infrared radiation. The underway data was acquired continuously and averaged to 30 second intervals on an HP9816 computer and recorded on 3.5 inch diskettes. These data were also transferred to 9 track tape upon return and processed on the IBM mainframe.

B. DATA CALIBRATION

Sensor calibration procedures are described in Jessen et al. (1989), but are briefly stated here for convenience. The temperature, conductivity, and pressure sensors on the CTD and the temperature and conductivity sensors of the underway sampling system were calibrated shortly after the cruise. The pressure calibration was carried out using a Chandler Engineering dead weight tester as a standard. At 10 equally spaced pressures from 50 to 500 db, indicated pressures from the standard and the CTD sensor were recorded. The differences between recorded values were within the stated accuracy of the sensor (+/- 1.6 db), therefore no pressure correction was applied. The temperature calibration was done using a Seabird temperature sensor as a standard. This standard sensor is recalibrated by the manufacturer approximately every six months. A temperature bath of 70- 80 liters of fresh water in an insulated tub was

used to compare the standard and sample sensors at 1° C increments from 0° - 20° C. 30 data points were collected at each temperature and then averaged to yield a single value for each sensor. A regression analysis was run on the 21 data points revealing a linear difference between the standard sensor and all of the sample sensors. The coefficients for the correction to the CTD temperature sensor were 1.00020 (slope) and +0.02361 (intercept). The best fit for the Seabird temperature sensor used in the underway sea surface temperature was linear with a slope of 1.0027 and an intercept of +0.0087. The relationship between the resistance of the Rosemount thermistor used for measuring sea surface skin temperature and the reference sensor was also linear with a slope of 2.568 and an intercept of -256.865. The accuracy of the temperature sensor was ± 0.003 °C with a precision of ± 0.0005 °C based on the specifications of the Sea-bird temperature sensor used as reference.

The conductivity calibration was carried out using a Guildline Model 8400 Autosal as a standard. The best fit for the Seabird conductivity sensor used in the underway system was a linear correction with coefficients of 1.0027 (slope) and +0.0087 (intercept). The accuracy of the salinity sensor was ± 0.003 psu with a precision of ± 0.002 psu based on the typical standard deviation of residuals in calibration.

After the raw CTD data were transferred to the IBM 3033 mainframe computer at the Naval Postgraduate School, the described temperature and conductivity corrections were applied to produce profiles of corrected pressure, temperature, and conductivity. Salinity was calculated from these corrected values according to the algorithm of Lewis and Perkins (1981). Severe spiking due to system malfunctions was eliminated from the salinity signal with a search for vertical salinity gradients greater than 1.0 PSU/m. Points that were determined to be bad were replaced using linear interpolation. Finally the data sets were averaged within 1 m intervals and visually examined for any remaining outliers missed during processing. If found, these points were replaced with linearly interpolated values. The accuracy of the pressure sensor based on the specifications of the Chandler Engineering dead weight testor was ± 0.1% of full scale with a precision of ± 0.05% of full scale.

C. AVHRR IMAGE PROCESSING

An important aspect of this study was the collection of NOAA 9 advanced very high resolution radiometer (AVHRR) data. NOAA 9 operates in a near-polar sun-synchronous orbit at a height of 850 km providing global coverage roughly twice daily. The AVHRR has a 1.1 km spatial resolution and is a five-channel device viewing in the visible (VIS 0.58-0.68μ), Near infrared (NIR .725 - 1.1μ), infrared (IR 3.55-3.93μ), (IR 10.3-11.3μ), and (IR 11.5-12.5μ) for channels 1 through 5 respectively. Channels 4 and 5 were predominately used since ocean structure is generally easier to detect in these frequency bands than in the lower ones. This is because a moist atmosphere is more transparent at 10.3μ and 11.5μ. The NOAA9 data were down linked and processed at the Scripps Satellite Oceanography Facility (SSOF) in La Jolla California. The raw data were transported to the Naval Postgraduate School on nine track tape and processed in the Interactive Digital Environmental Analysis (IDEA) Lab.

All of the imagery were navigated using the AVIAN AVHRR Navigation Program of the Transportable Applications Executive (TAE) on the IDEA Lab VAX 11/780 computer at the Naval Postgraduate School. This program is a six step operation to convert a raw image to a navigated enhanced image. The first step in this procedure is to GLEAN the tape. This allows the computer to scan the image for satellite timing, orientation, and track information and to check the length of the raw image file. The next step is OVERVIEW. This provides a quick look at the full pass by displaying every eighth pixel and line. The third step is CALIB. This adjusts the pixel intensity for the instrument and the sun angle. This fifth step is called PICKEM which allows the user to pick out up to sixteen landmark areas for navigation purposes. This procedure yields position accuracies of ± 3 km with a precision of ± .5 km. The final step in the procedure is called REALMAP. This subroutine allows the user to pick a channel to be displayed and the minimum and maximum temperatures for pixel values. The minimum value is the quantity displayed as zero (black) and the maximum is the quantity displayed as 252 (white) The pixel values less than the minimum are displayed as black and more than the maximum as white. Values in between are mapped to gray shades linearly. For the purpose of this study

the SST algorithm was used which has default temperature range of 273.16° K to 293.66° K. This algorithm is a split-window (day) function as described in McClain et al., (1985), which uses a combination of channels 4 and 5 to best bring out the oceanographic features. The accuracy of this function is ± 0.5° C with a precision of ± 0.1° C. The remotely sensed sea surface temperature field was obtained using the PIXVAL function of the DIPS program and the *in-situ* data were processed and contoured using the primary data processing programs (GEMPAK) in the IDEA LAB.

D. TRANSPORTABLE APPLICATIONS EXECUTIVE (TAE)

All of the subroutines used are part of the Display Management Subsystem (DMS) of the (TAE). The DMS supports the development of device-independent image display software. It gives the user the ability to make image display applications easier to develop and more portable among different image display devices. Each display has a number of memory planes that are use to store image data and a number of graphics planes that are used to store and display graphics data. The image data in the memory planes represent gray levels, which are then mapped (or translated) through look-up tables to obtain intensities that are displayed on the color monitor. Pointing devices give the user the capability to interact with the color monitor.

The display can be thought of as a stack of two-dimensional planes. The resolution of the display is defined as the number of lines and samples that can be stored in a memory plane. Each pixel in the memory plane can have a value ranging from 0 through 255. The data in each memory plane are viewed on the display. When image data are loaded into a display, each specified band is resampled if necessary and stored in its own memory plane. All DMS functions that display, manipulate, or analyze image data reference these memory planes.

Each pixel in the memory plane corresponds to a specific spot on the color monitor. At each spot is a group of three phosphors: a red, a green, and a blue light-emitting phosphor. The color and intensity of each spot on the monitor is a result of the combination of the amount of light emitted by the red, green, and blue

phosphors at that spot. The same amount of light emitted by the three phosphors at a spot will combine to produce a shade of grey at that particular location, which is how black-and-white images are displayed on a color monitor. An image is displayed on a monitor by using the data in the memory plane(s) to control the color and intensity of the spots on the monitor.

The graphics planes are similar in organization to memory planes except that each pixel of a graphics plane does not hold a value between 0 and 255 but rather a value representing 0 or 1, which represent an "on" or "off" state. The information stored in graphics planes can be shown in a number of colors depending on the display type. Graphics planes are mostly used as an overlay to an already displayed image. They are used to display mensuration data--annotation, polygons, lines, or points--and to display histograms of either the image data or the look-up table applied to the image data.

Pointing devices give the user the capability to interact with the color monitor by moving a cursor over the monitor. These devices included trackballs, joysticks, mouses, or light pens.

1. Gempak Processing

The *in-situ* data sets were processed using GEMPAK subroutines in three steps. First the data had to be converted to a format resembling an upper air format which the GEMPAK subroutines recognize. This was done using a simple output conversion of the oceanographic data. Next the data set had to be formatted into an upper air GEMPAK file. This was accomplished using the UPPER AIR subroutine within GEMPAK which converts a raw sounding into a GEMPAK file. The final step was to convert this upper air sounding file into a gridded data set by using the Objective Analysis (OABSND) subroutine. This step performs a Barnes objective analysis on the sounding data and can analyze several parameters at one time. Each pass of the analysis interpolates data from station grid points using the weighting function:

$$WTFUNC = [EXP(DIST**2/WEIGHT]$$

where:

DIST**2 = [(lat(grid)-lat(stn))**2 + (lon(grid)-lon(stn))**2] *(COSLSQ(grid))

COSLSQ = cos(lat(grid))

WEIGHT = 5.051457 * (DELTAN*2/PI)**2

DELTAN = Station spacing read from grid file analysis block

This output is a grid matrix with variable grid-area parameters. Therefore the smallest gridsize to cover the data points was used to obtain the best possible resolution. Data set two for the 1987 cruise had to broken into two separate sections due to the awkward shape of the sampling scheme which was best approximated by two adjacent rectangles. The other 2 data sets were further offshore and could be gridded as one entire set.

2. Display Image Processing System (DIPS)

After completion of the navigation process the images were enhanced to allow the best temperature resolution within the range common to the waters offshore from California. The enhancement scale had a range of pixel values from 0 to 255 with 0 representing 8° C and 255 corresponding to 18° C. The temperature scale was incremented every .5° C and the pixel values every 16 units.

The sea surface temperature field was obtained using the pixel value determination subroutine (PIXVAL). After overlaying the station positions of the *in-situ* data on to the appropriate satellite image, the pixval cursor was maneuvered over the cross haired position marker. The pixel value of this point was obtained. Then a three by three pixel average (nine points total) was taken around the station position to obtain the sea surface temperature average for each station. A similar procedure was used by Simpson et. al., (1986).

E. CORRELATION COEFFICIENT DETERMINATION

The normalized vertical correlation coefficient between the AVHRR imagery and each subsurface in-situ data station was obtained using the following correlation function (Walpole and Myers, 1985):

$$r(z) = \frac{\sum_{i=1}^{n} \phi_i \psi_i(z)}{\left[\sum_{i=1}^{n} \phi_i^2 \sum_{i=1}^{n} \psi_i^2(z) \right]^{\frac{1}{2}}} \qquad \text{(eqn. 1)}$$

where z is the depth, n is the number of hydrographic stations, ϕ_i is a remotely sensed (surface) field, and $\psi_i(z)$ is an *in-situ* subsurface field. This function is similar to that used by Simpson et. al., (1986) and Van Woert, (1982), except that the one used here has both input parameters demeaned. The sub-surface temperature field was obtained by creating a sounding file for the particular depth of interest within the (upper air) subroutine of GEMPAK. This allowed for a much easier array to manipulate and allowed the removal of any shallow stations which did not contain the depth of interest. The remotely sensed data set could then be easily changed to match the positions of the altered *in-situ* temperature array.

F. SIGNIFICANCE LEVEL DETERMINATION

The ninety-five percent level of significance was determined by computing the autocorrelation of the remotely sensed data. This was accomplished by generating a standard seven by nine grid matrix from the 1988 data stations. The SST's from the missing CTD stations (Figure 3) were determined from the pixel values obtained from the satellite image. The overall area of the grid matrix was divided by the positive area (that greater than the first zero crossing) of the autocorrelation function (Figure 4). The result, n, was used as the reduced number of degrees of freedom. This technique is an extension of the method used by Beardsley et. al. (1985) to determine the number of real degrees of freedom for correlated time series. This value was applied to the standard level of significance formula (Miller and Freund, 1985):

$$z = \sqrt{n - 3}\, Z \qquad \text{(eqn. 2)}$$

Where:

Where:

$$Z = \frac{1}{2} \ln \frac{1 + r}{1 - r}$$

r = correlation coefficient

to determine the correlation value which was the 95% significance level.

Correlations for the (CTZE87) cruise were divided into three sections. The first section covered the overall area using data set number one with the remotely sensed field being obtained from the NOAA9 image from the 16th of June. The second data set covered the coastal areas and the small scale "squirt" off of Point Arena and was correlated with the image from the 21st of June. The third data set was centered over the large offshore filament and was correlated with the image from the 27th of June.

The correlation for the 1988 data was divided into 2 sections covering the first and second half of the cruise. Another data set was also created for each half using only the stations located in the strong offshore filament. This allows a comparison of the changes in the vertical extent of the filament with time and space.

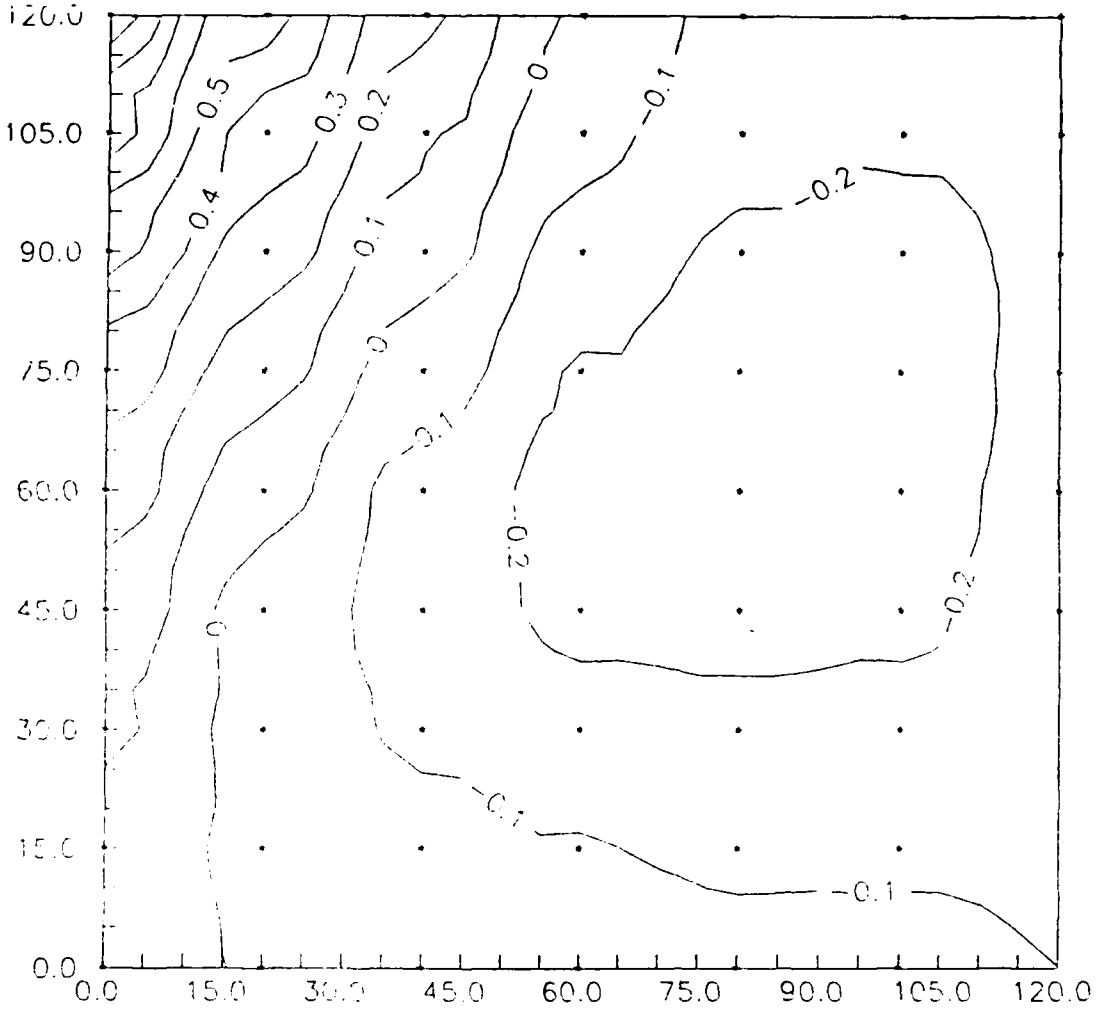

Figure 4 Autocorrelation function of gridded AVHRR derived SST field (July 09, 1988).

III. RESULTS

A. 1987 CRUISE RESULTS

Analysis of the (CTZE87) first data set (Stations 1 - 54) yielded a positive correlation from the surface (.86) to 85 m (.81). Below this level the correlations slowly dropped off to (.50) at a depth of 132 m (Figure 5). The correlation continued to decrease with depth and actually became negative (-.09) at a depth of 250 m. The negative correlation continued to increase with depth and reached a maximum of -.42 at a depth of 500 m.

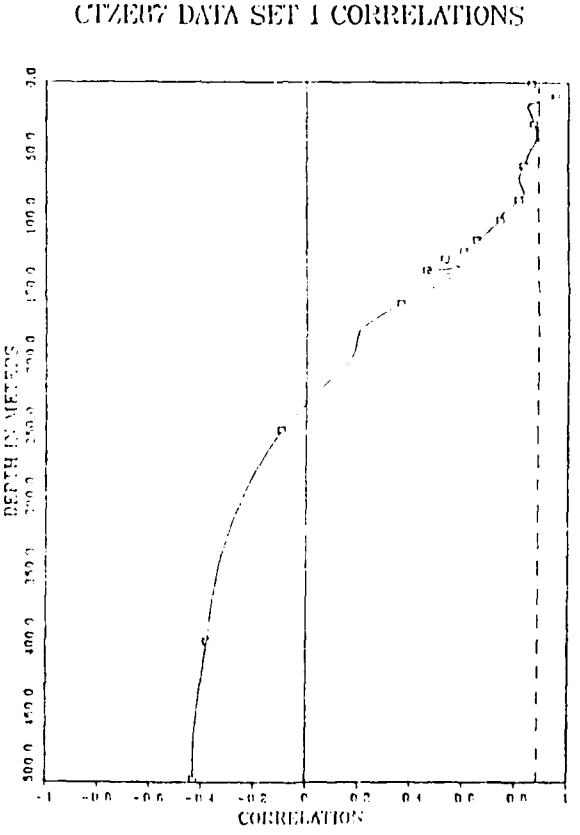

Figure 5 Correlation coefficient between AVHRR derived SST and *in-situ* temperature field as a function of depth (June 16, 1987).

The 95% level of significance is indicated as the dashed line on Figure 5. The level of highest correlation did not occur at the surface (.86) but occurred at 40 m (.88) which was also the best match visually between the AVHRR imagery and the 40 m temperature contours (Figures 6 and 7). The correlation between the imagery and the surface dynamic height relative to 500 db yielded (.36), which was not statistically significant (Figure 8).

The second data set (Stations 55-78) had a slightly higher positive correlation at upper levels above 50 m with the exception of the surface (.69) down to 3 m (.75) (Figure 9). The highest correlation level was at 30 m (.93) which was also a very good visual match (Figure 10). The correlation dropped below the 95 percent significance level at 80 m (.54) and went negative (-.05) at 120 m. There were no significant changes below this depth with the correlation fluctuating from values just slightly above to just below 0.

The third data set (Stations 79-115) for the 1987 cruise had much poorer correlations with the maximum occurring at 40 m (.70), (Figure 11). The correlations decreased to .25 at the surface and -.01 at 150 m. The author feels these levels were so much lower than the first two data sets because of the temporal offset between the satellite image and the sampling time frame. The closest AVHRR imagery to the data was on the 22nd of June due to the fact that the image on the 27th of June had extensive cloud cover with no visible oceanographic features. The imagery on the 22nd was very good but was 3 days before the mid-point of this phase of the cruise, yielding much lower correlations (Figure 12). Three days were apparently sufficient time for significant temporal changes to occur in the filament, and the data became decorrelated.

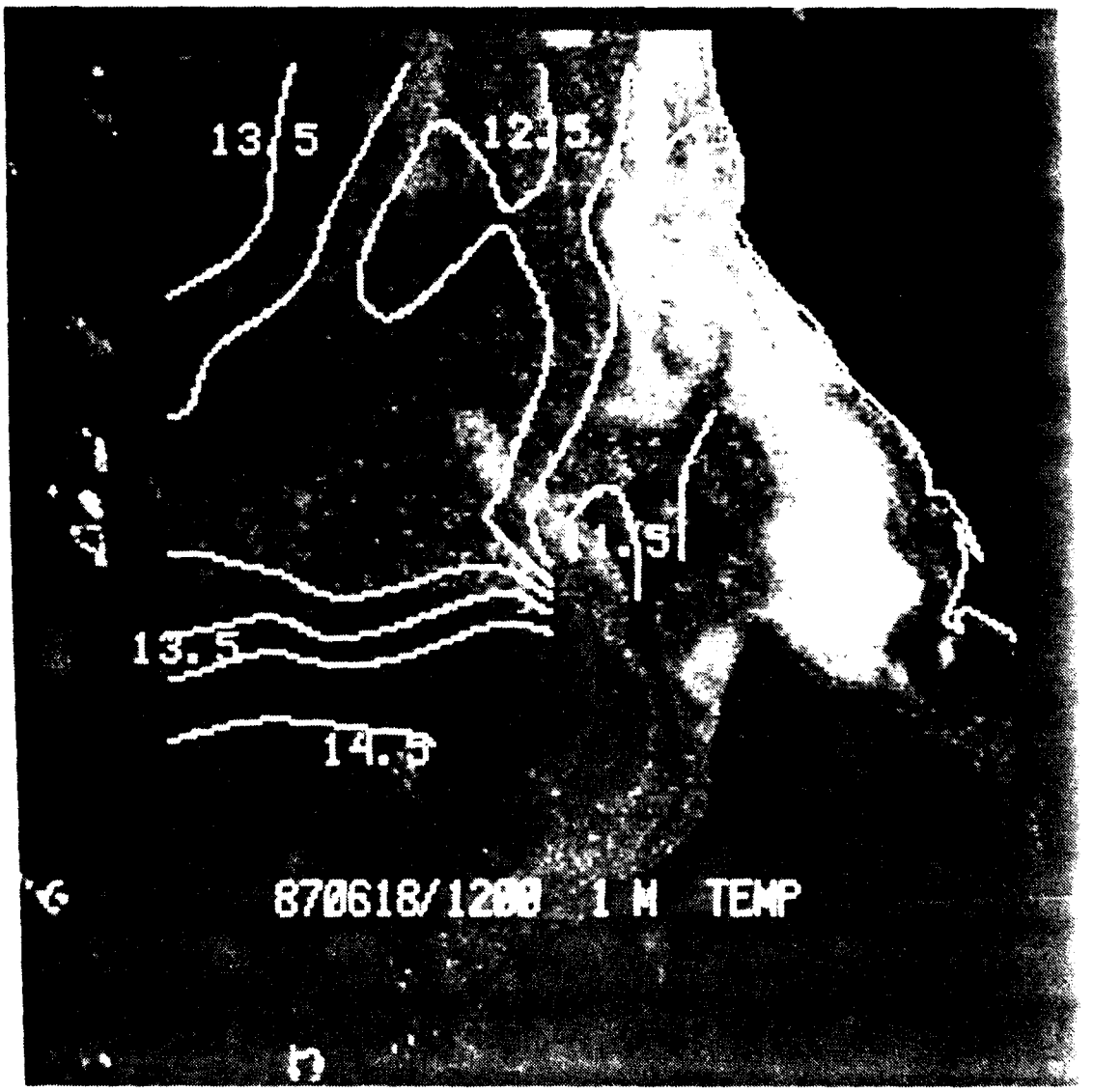

Figure 6 AVHRR imagery for June 18, 1987 with 1 m temperature contours from the *in-situ* (CTD) data.

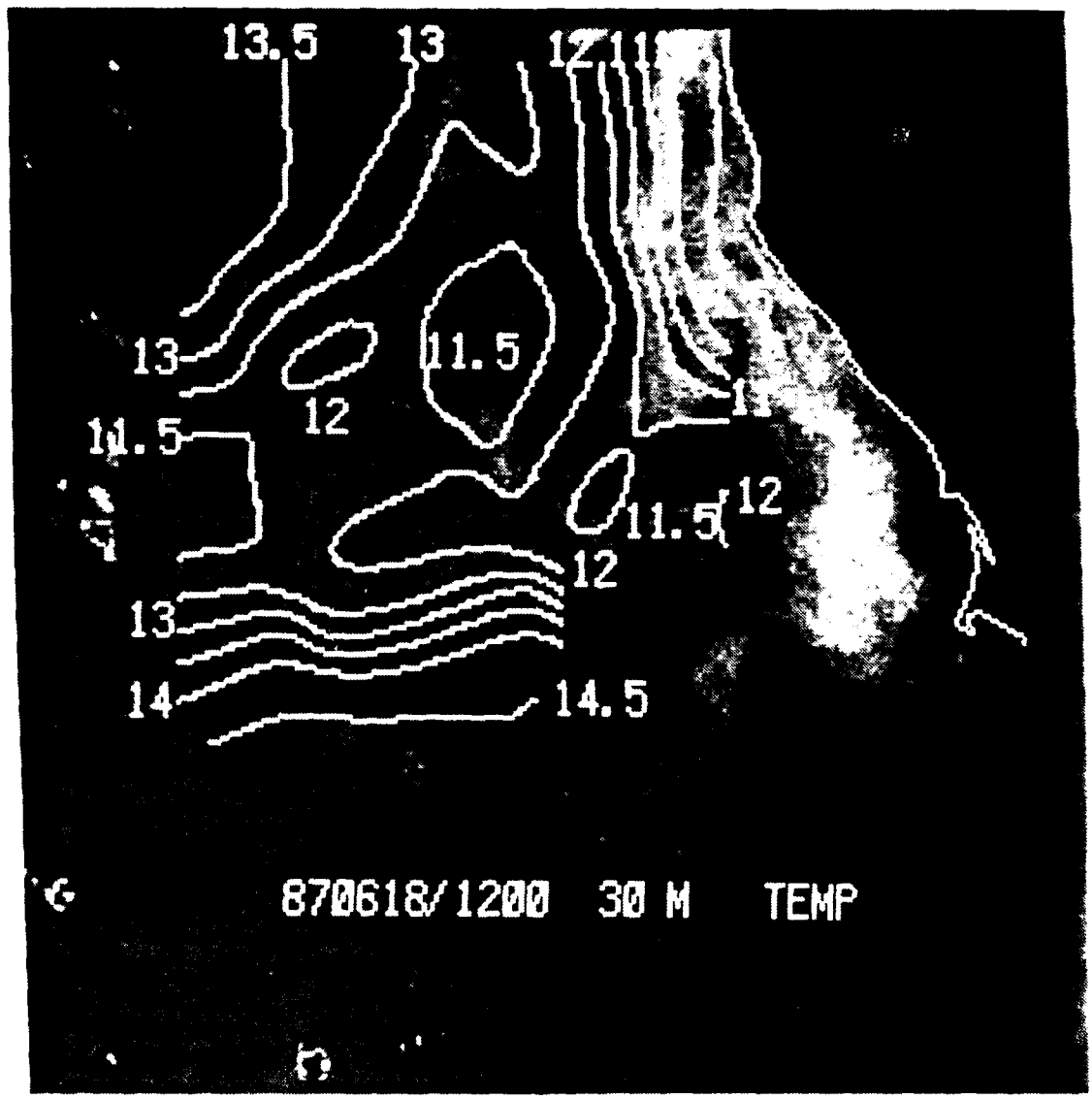

Figure 7 AVHRR imagery for June 18, 1987 with 30 m temperature contours from the *in-situ* (CTD) data.

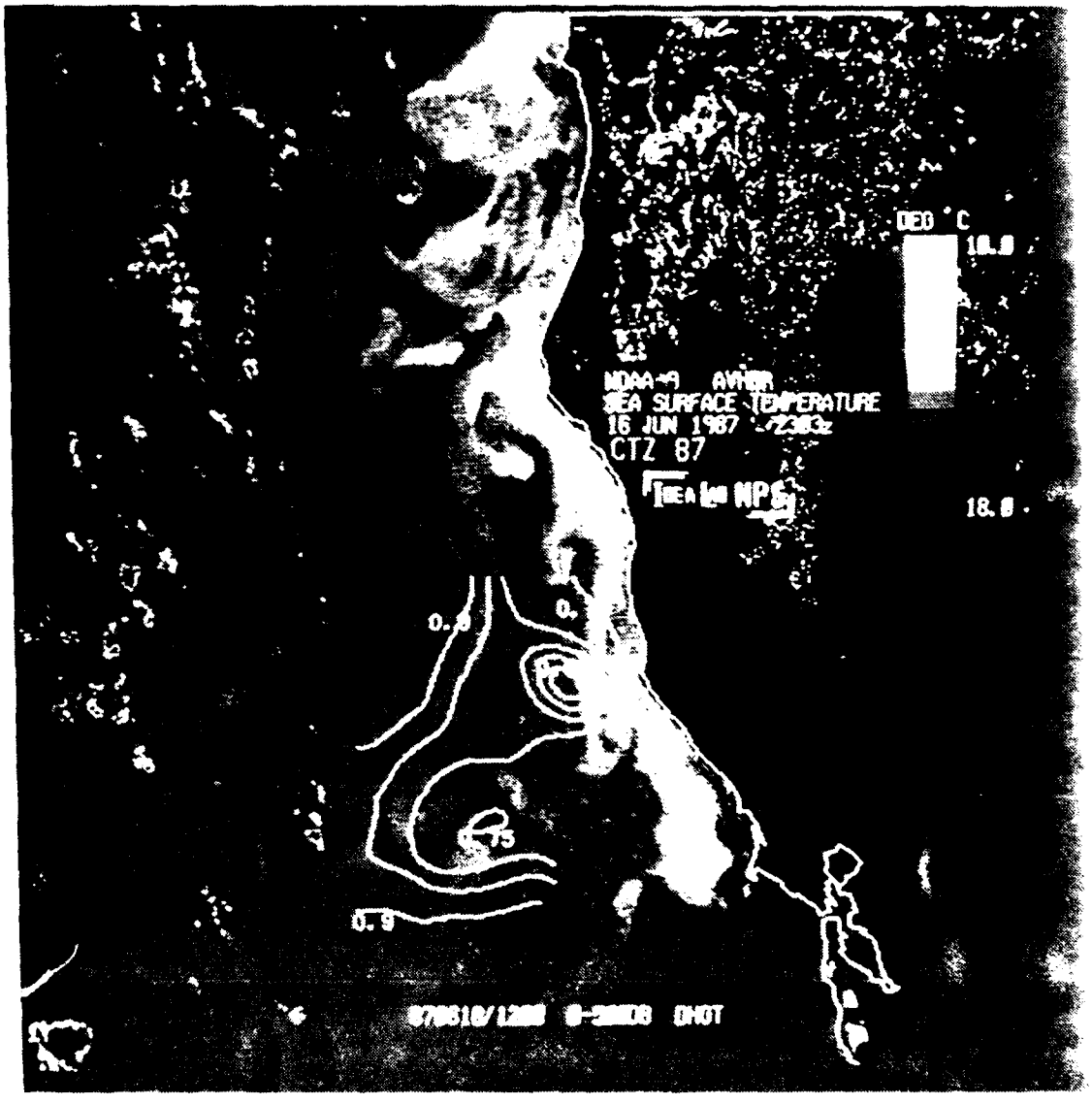

Figure 8 AVHRR imagery for June 18, 1987 with Surface Dynamic Height contours referenced to 500 db.

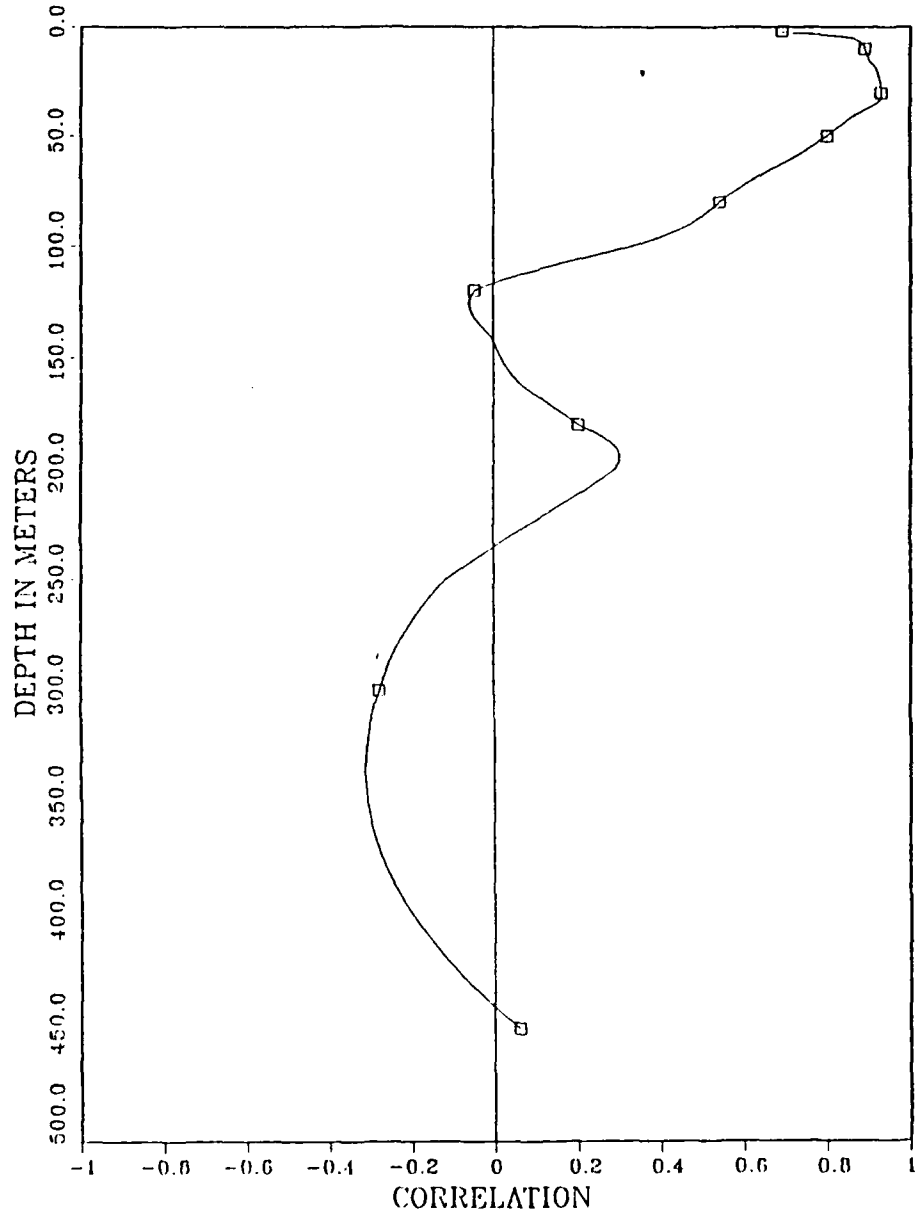

Figure 9 Correlation coefficient between AVHRR imagery derived SST and *in-situ* temperature field as a function of depth (June 21, 1987).

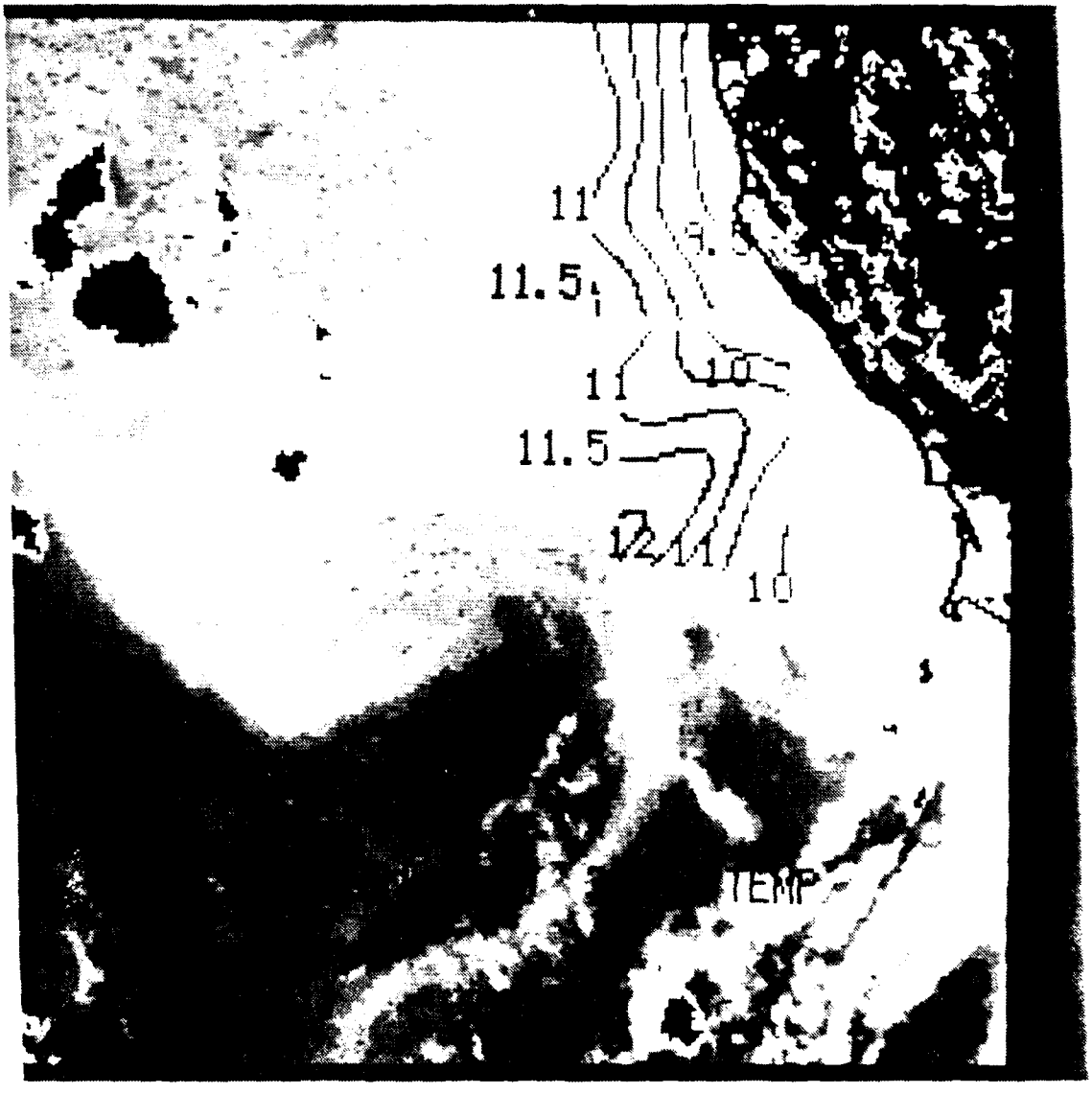

Figure 10 AVHRR imagery for June 21, 1987 with *in-situ* temperature contours at 30 m depth.

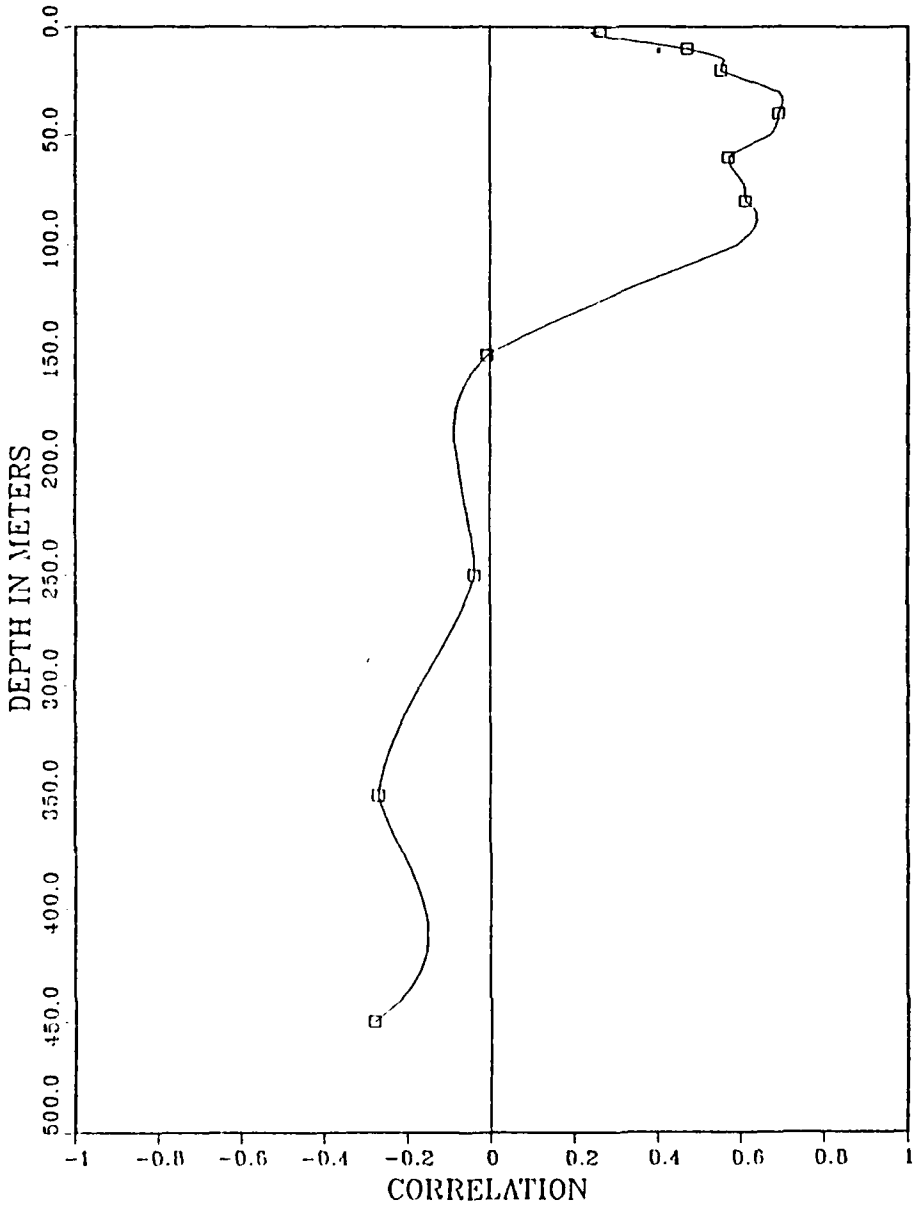

Figure 11 Correlation coefficient between AVHRR imagery derived SST and *in-situ* temperature field as a function of depth (June 27, 1987).

Figure 12 AVHRR imagery for June 22, 1987 with *in-situ* (CTD) temperature contours at 40 m.

B. 1988 CRUISE RESULTS

The first data set for the 1988 cruise consisted of 58 stations which was broken into two sets, the first covering the overall area (all data) and the second covering only those stations located in the strong offshore filament. The full data set yielded correlations of (.89) from the surface down to 30 m (Figure 13). The correlations began slowly decreasing to .71 at 150 m and .61 at 250 m. The most significant drop occurred between this level and 300 m where the correlation dropped to (.44). The positive correlation continued to decrease and became negative at the 380 m level and continued to decrease to a minimum of -.40 at 490 M. Visually the 1 m temperature contours match well with the image except that the filament was offset to the south in the in-situ data. This is attributed to the time lag between the image and the data sampling (Figure 14). The 40 m temperature contours are very similar to the 1 m plot showing the same southerly offset (Figure 15).

There were 18 stations chosen for the filament sub-set. These were the stations located within or just on the outer wall of the filament as determined both from the imagery and verified with the 1 m temperature from the in-situ data. The station numbers used were the following: 07, 08, 09, 10, 11, 15, 16, 17, 25, 26, 36, 37, 41, 42, 55, 56, 60, and 61 (Figure 3). The correlation ranged from .70 at the surface to .75 at 10 m and then slowly decreased to .59 at 50 m. It decreased more rapidly at this point down to .40 at 150 m. This data set also became negative at 380 m and followed the negative trend down to 500 m (-.20) (Figure 16). Comparing this to the profile obtained using the overall data set (Figure 13) it can be seen that the subset profile overall has a lower correlation coefficient by an average of (.2) down to 250 m. Below this depth both curves are similar.

The second half of the 1988 cruise consisted of 56 stations with some of the northerly stations not sampled due to the same reasons discussed above. The correlations for this data set were strongly positive (.93) at the surface and at 20 m (.94). They slowly decreased to .60 at 200 m. Below this level the correlation began decreasing much more rapidly to .47 at 225 m and .08 at 300 m. The correlation became negative at 315 m and continued to become more negative to -.53 at 500 m (Figure 17). Visually the 1 m temperature contours matched the image better for this

half of the cruise with the filament being well defined by the contours (Figure 18). The temperature in the outer portion of the filament was actually 2°C colder than indicated on the plot which was a function of GEMPAK'S inability to contour parameters requiring a narrow closed contour. The first level below the 95% level of significance was 150 m. This level still shows an excellent pattern between the image and the temperature contours (Figure 19).

The filament sub-set for this half of the cruise consisted of 16 stations. The station numbers chosen were the following: 07, 08, 09, 10, 11, 15, 16, 17, 24, 25, 26, 37, 38, 41, 855, 56, and 61. The correlations were higher than the previous week at upper levels ranging from .80 at the surface and increasing to a maximum of .85 at 20 m. The correlation then slowly decreased to .59 at 200 m. Below this level the correlation dropped off dramatically going from .41 at 220 m to -.01 at 245 m. The data set remained negative to 500 m varying between -.1 to -.40 at 400 m (Figure 20).

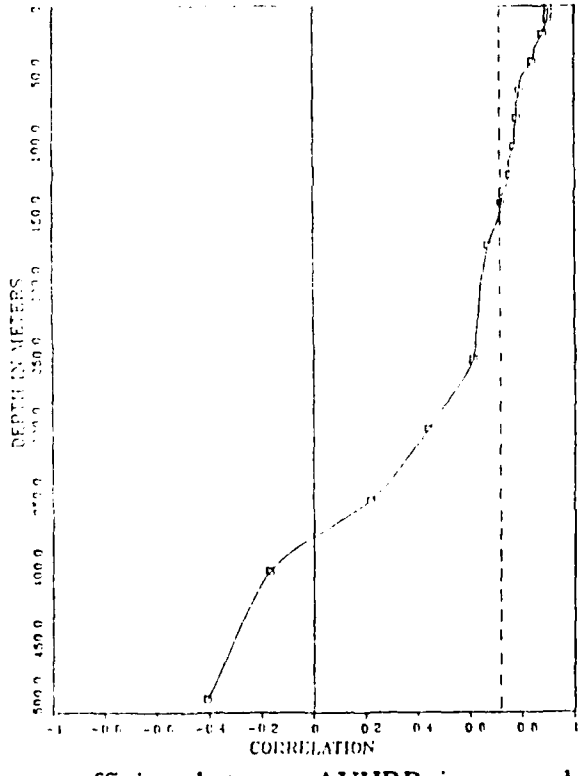

Figure 13 Correlation coefficient between AVHRR imagery derived SST and *in-situ* temperature fields as a function of depth (July 09, 1988).

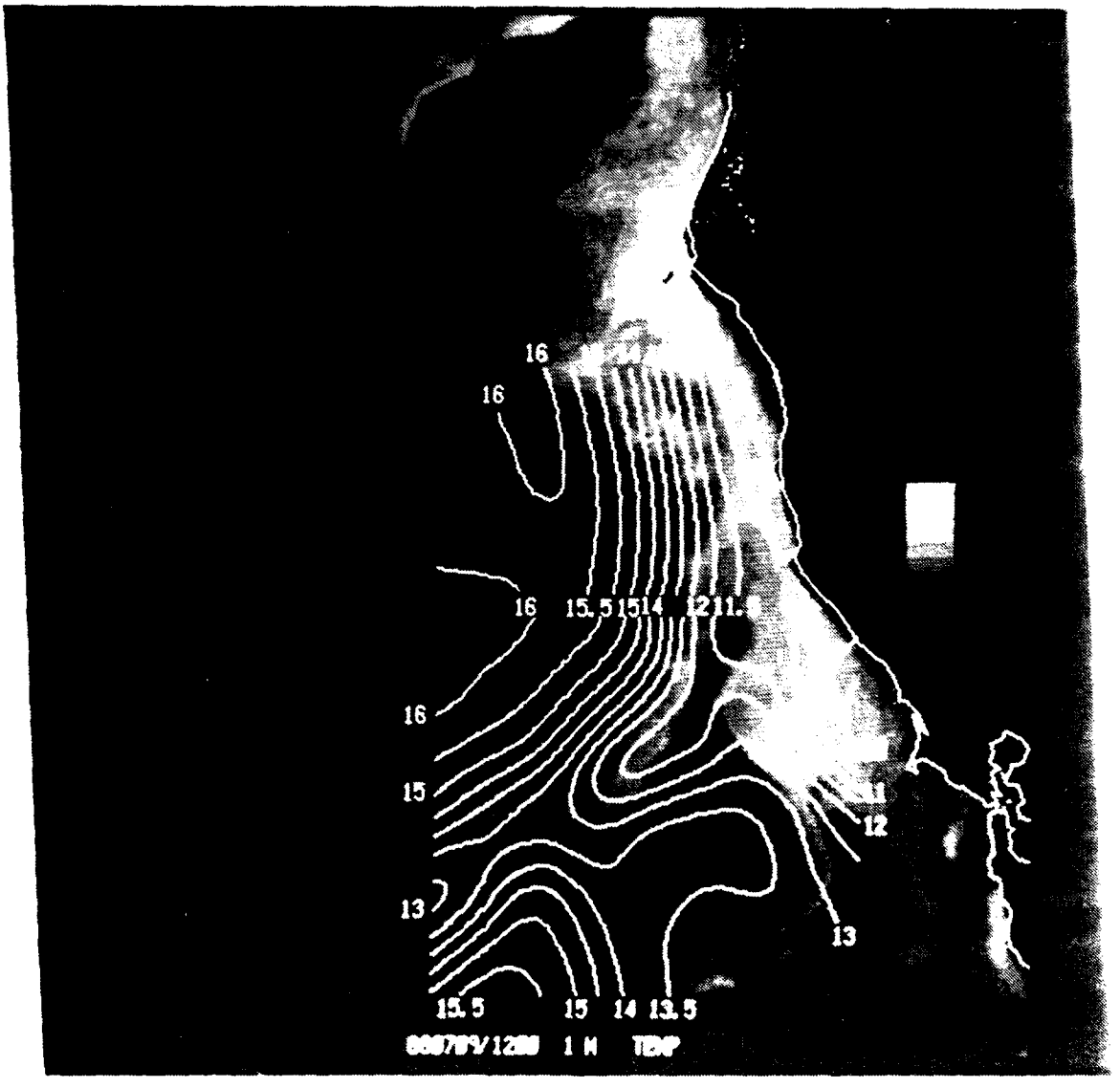

Figure 14 AVHRR imagery for July 09, 1988 with *in-situ* (CTD) temperature contours at 1 m depth.

Figure 15 AVHRR imagery for July 09, 1988 with *in-situ* (CTD) temperature contours at 40 *m* depth.

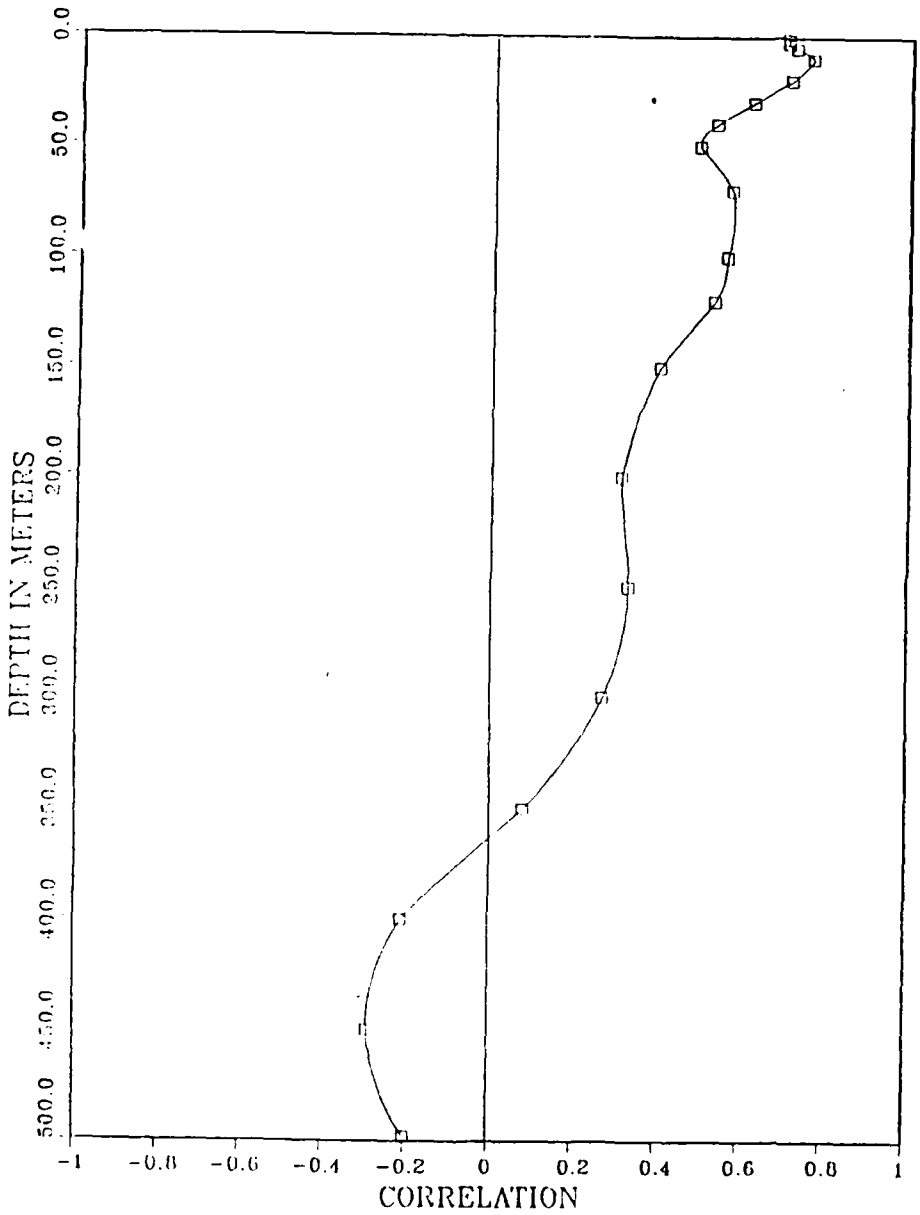

Figure 16 Correlation coefficient between AVHRR imagery derived SST and *in-situ* temperature fields as a function of depth (July 09, 1988 filament sub-set).

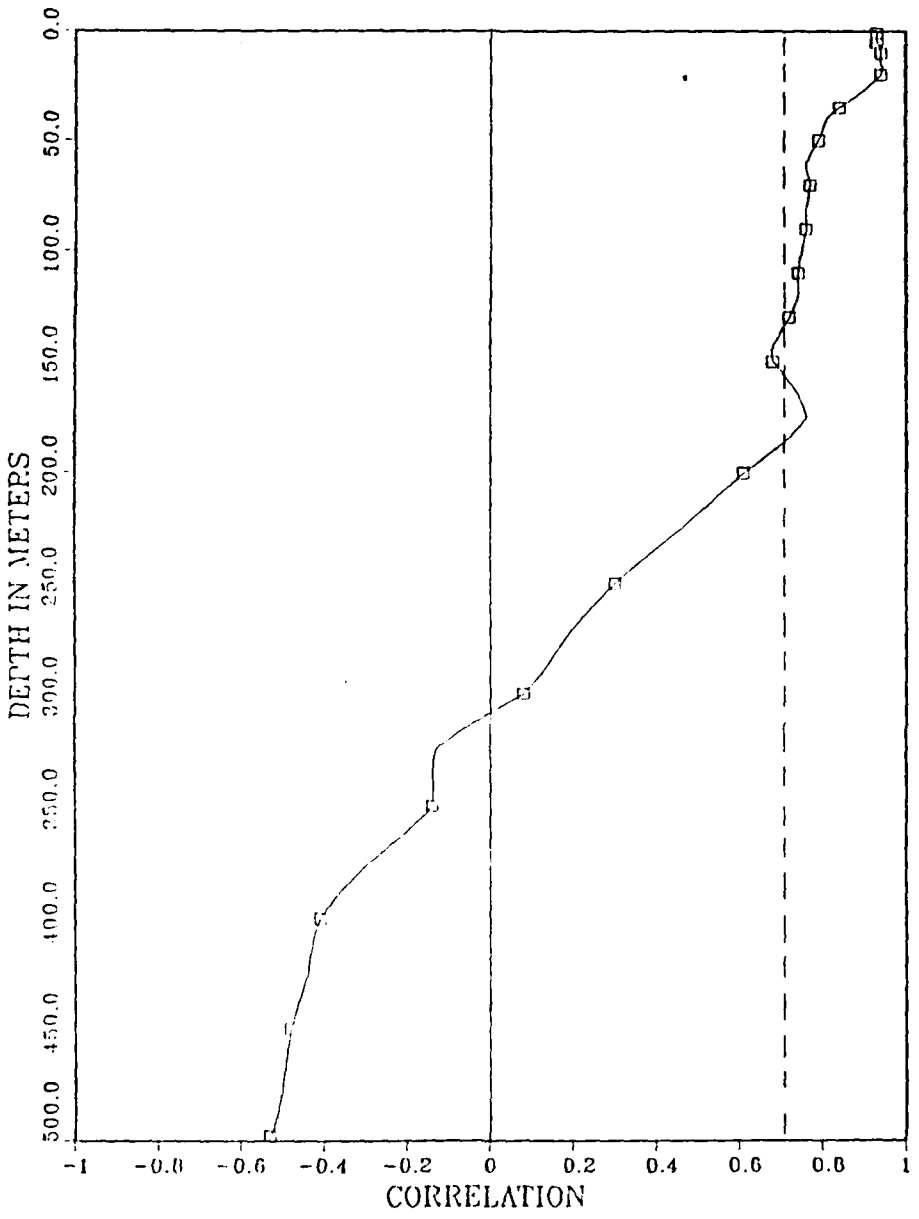

Figure 17 Correlation coefficient between AVHRR imagery derived SST and *in-situ* (CTD) temperature fields as a function of depth (July 16, 1988).

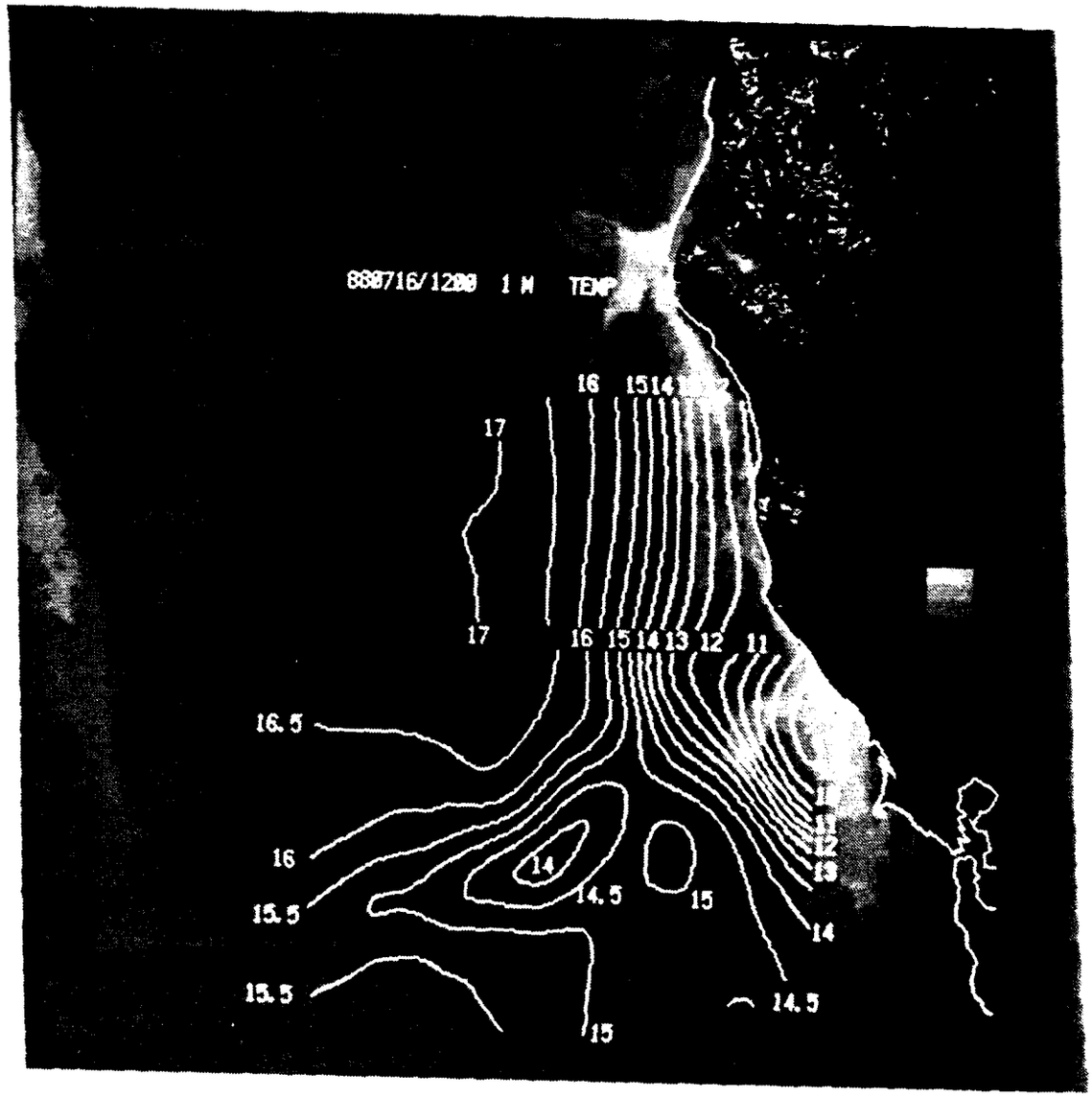

Figure 18 AVHRR imagery for July 16, 1988 with *in-situ* (CTD) temperature contours at 1 m depth.

Figure 19 AVHRR imagery for July 16, 1988 with *in-situ* (CTD) temperature contours at 150 m depth.

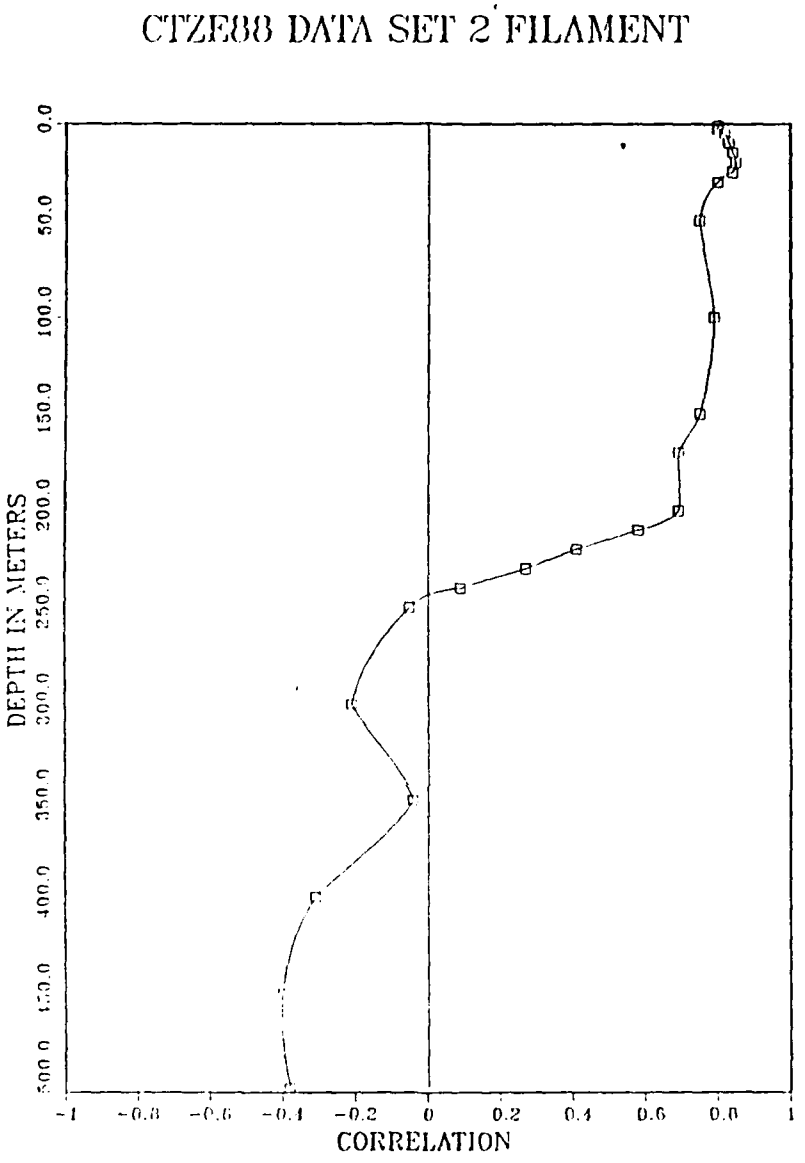

Figure 20 Correlation coefficient between AVHRR imagery derived SST and *in-situ* temperature field as a function of depth (July 16, 1988 filament sub-set).

Correlations were also obtained between the *in-situ* SST and the *in-situ* temperature field for the 1987 data. This was used to determine whether the sub-surface maximum was attributed to the temporal variability or if there were actually

some unexpected subsurface feature which the data detected. The results obtained support the former argument since the maximum for these data sets yield the highest positive correlations at the surface (Figures 21, 22, and 23).

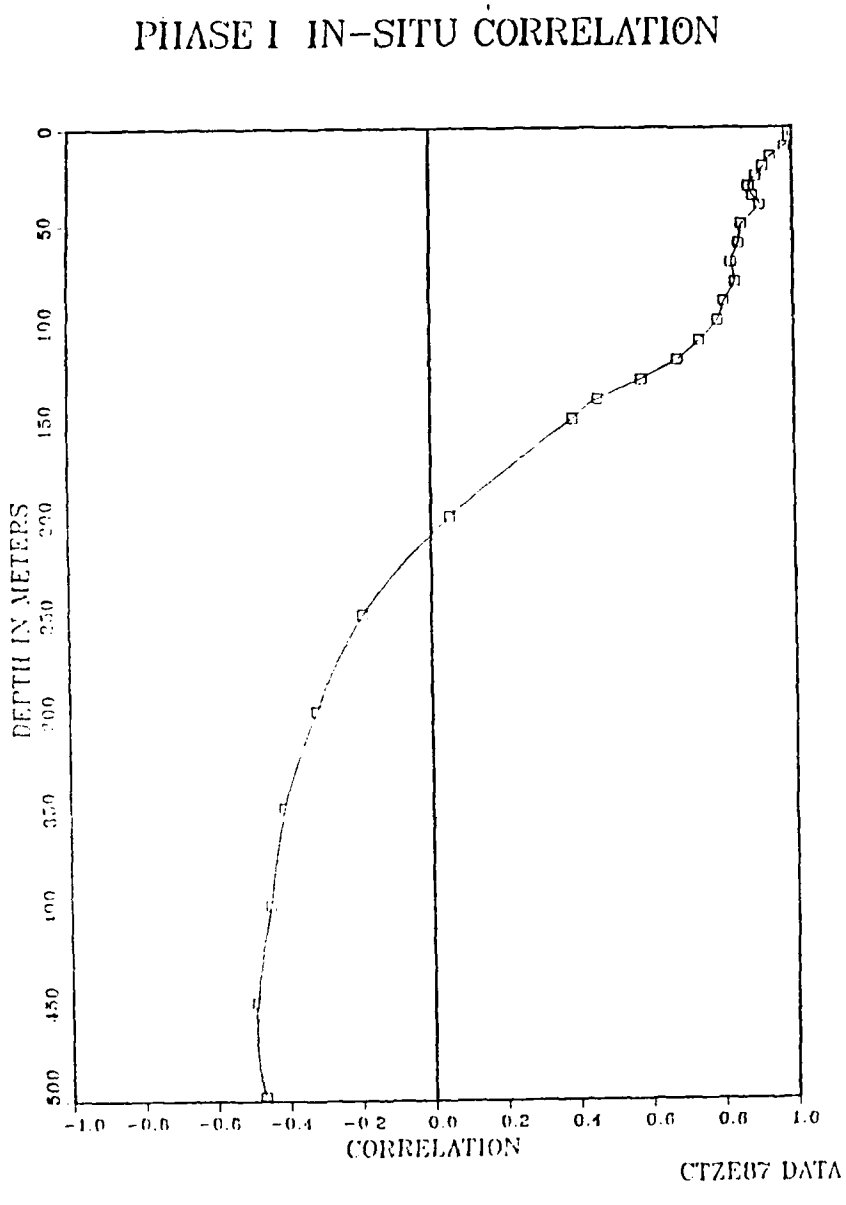

Figure 21 Correlation coefficient between *in-situ* SST and *in-situ* temperature field as a function of depth (June 16, 1987).

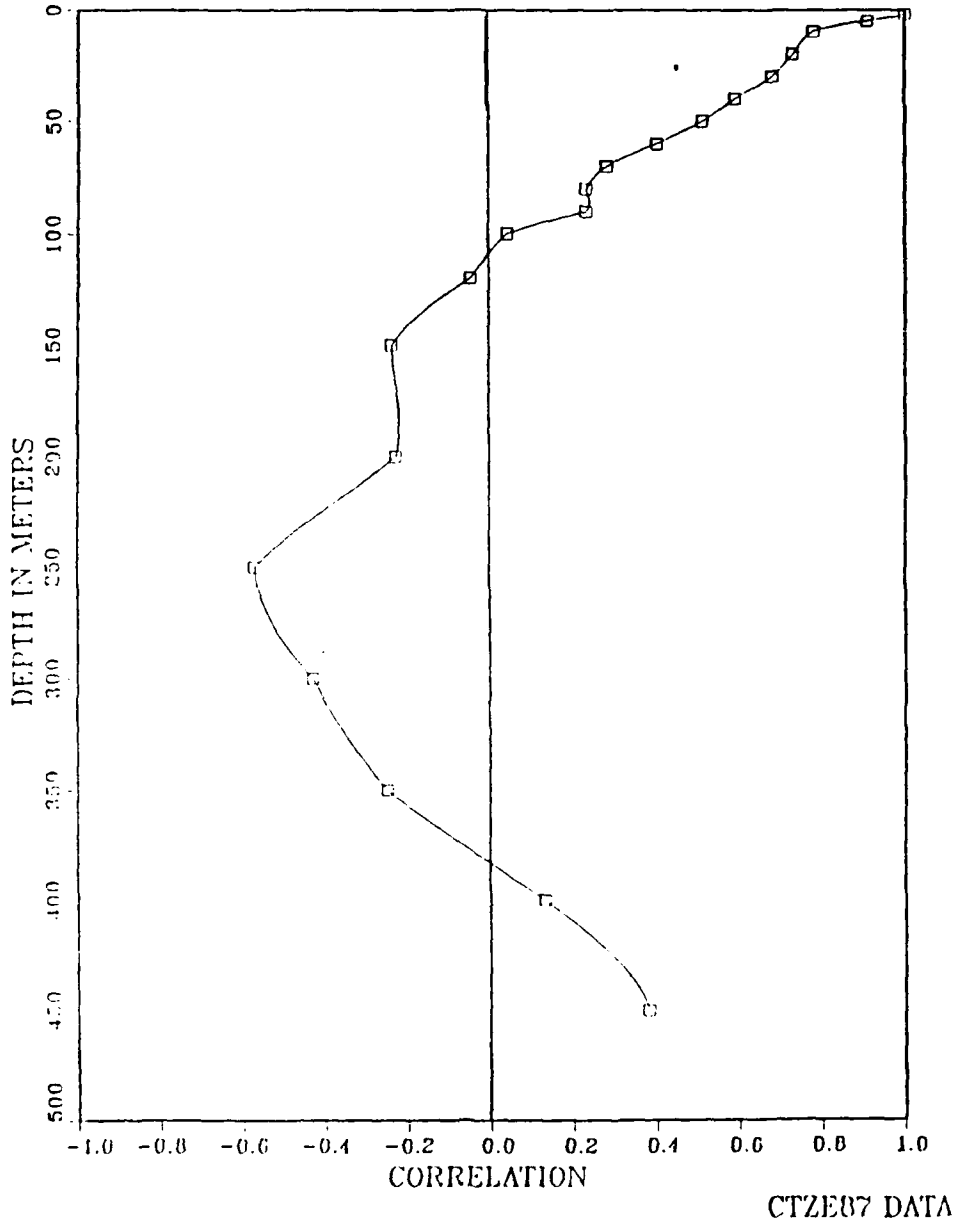

Figure 22 Correlation coefficient between *in-situ* SST and *in-situ* temperature field as a function of depth (June 21, 1987).

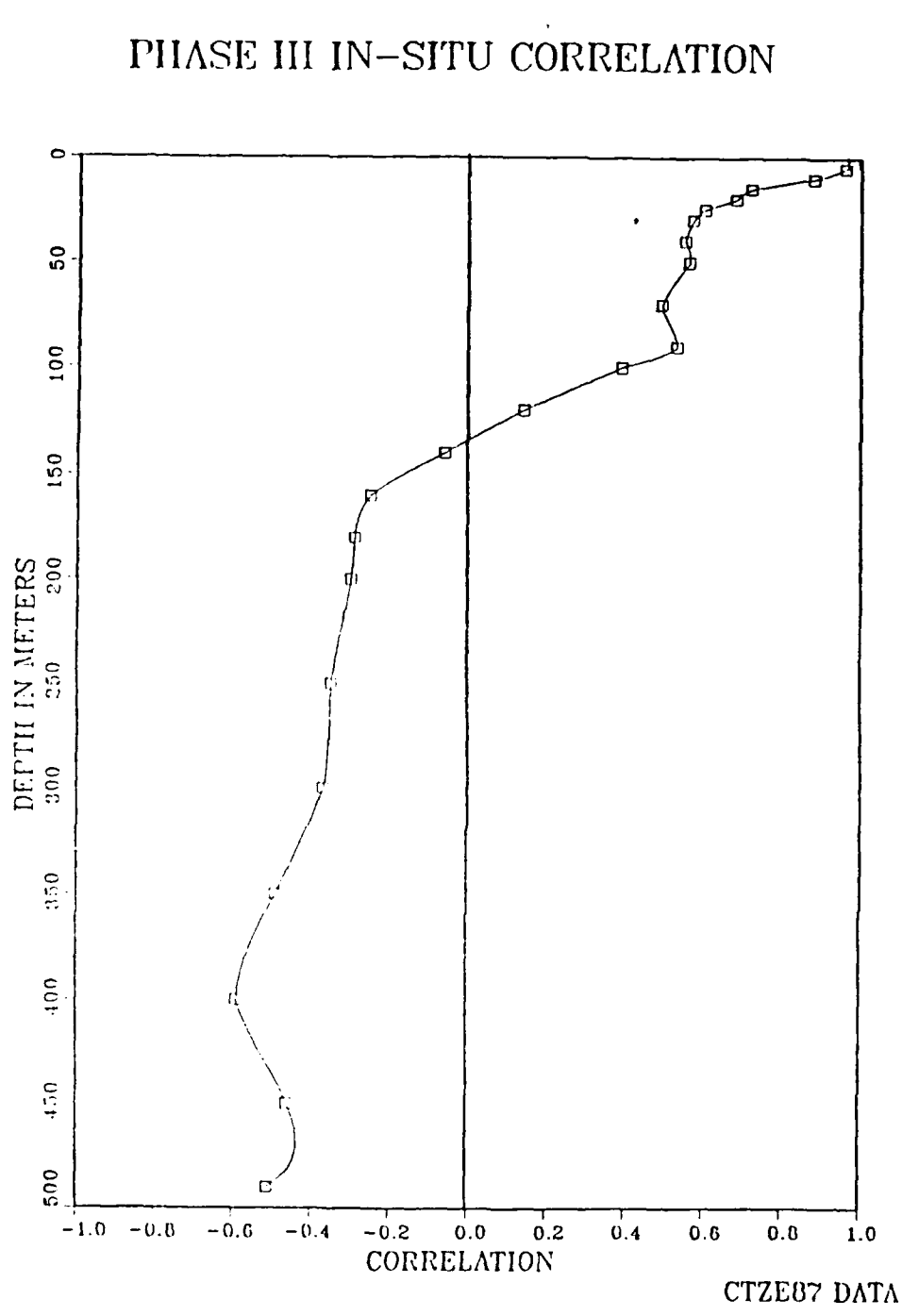

Figure 23 Correlation coefficient between *in-situ* SST and *in-situ* temperature field as a function of depth (June 28, 1987).

IV. DISCUSSION

A. AVHRR AND *IN-SITU* SST COMPARISON

The comparison between the AVHRR image derived and the *in-situ* SST fields varied greatly between each data set. The plot for June 16, 1987, shows that the AVHRR SST overestimated the temperature by an average of 3°C, (Figure 24). A linear regression curve of this set indicates no biases on either the high or low end of the temperature spectrum. The overestimation is the result of a problem with Channel 5 on the NOAA-9 satellite. This channel was presenting a grainy image detracting from the resolution of the image. After removing this channel from image only channel 4 was being used and this is a non-calibrated channel. The temperature gray shade scale of this image is still linear but the temperature end points appear to be approximately 3°C too high.

The second phase data set showed a linear trend with the AVHRR SST slightly higher than the *in-situ* temperature (Figure 25). The third phase had greater variability than the first two phases with the temperatures varying 0°C to 3°C with no indication of an over or underestimation by either the AVHRR SST field or the *in-situ* field. The images used for these two phases of the cruise were from the NOAA-10 satellite and did not have the problem of the image from the first phase. The 1988 data comparison shows a greater degree of variability ranging from 0°C to 3.5°C, (Figure 26). It also shows an underestimation by the AVHRR SST field at the high end of the temperature field.

These figures indicate much more scatter than expected (up to 3.5°C) as compared with the resolution of the image (.1°C). This is attributed to the temporal variation between the image and the *in-situ* sampling period. A more efficient way to compare satellite sensed versus *in-situ* data would be to have a synoptic data collection process (such as a floating buoy time series) which allows comparisons to be made which are exact in space and time.

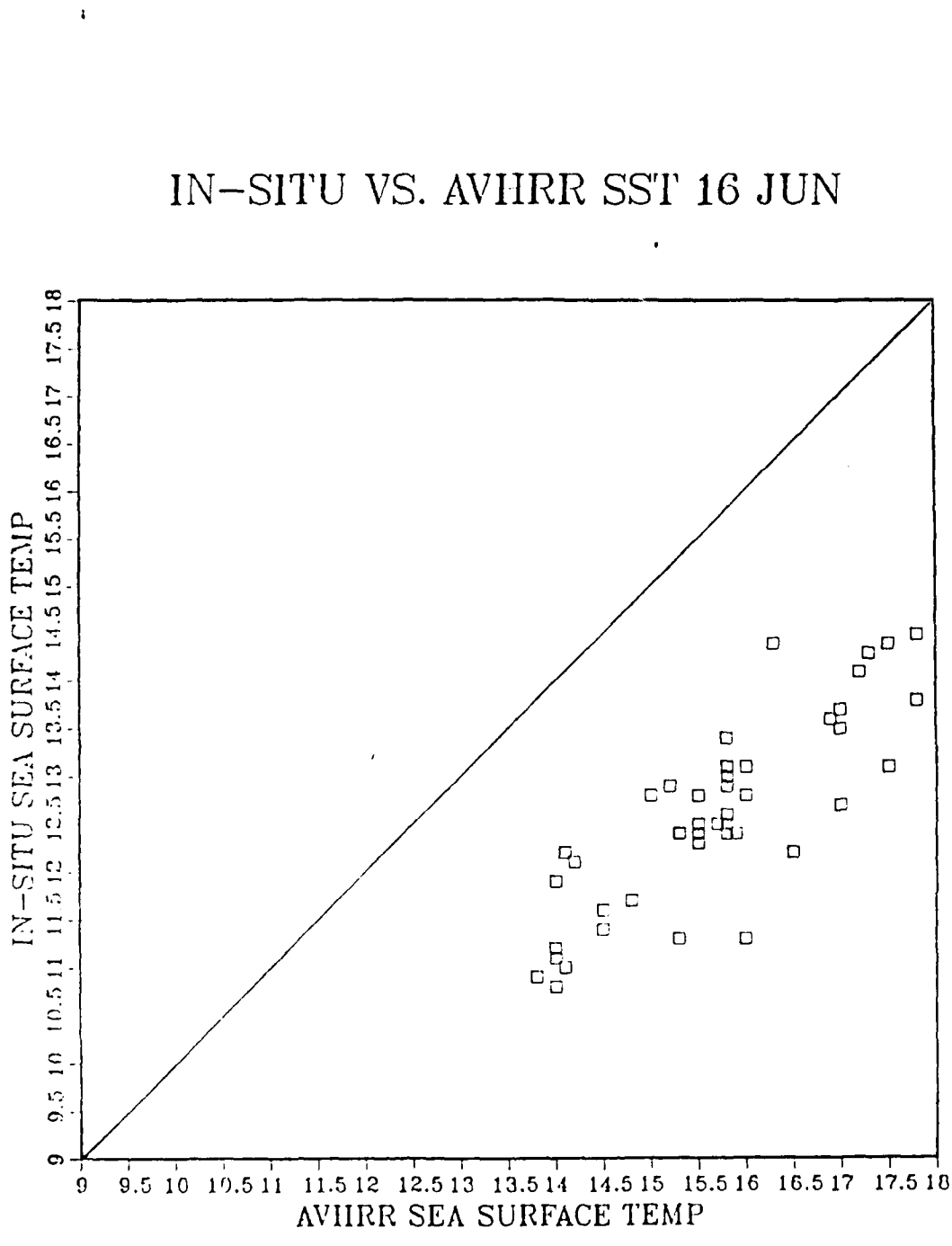

Figure 24 AVHRR versus *In-situ* SST Comparison for June 16, 1987.

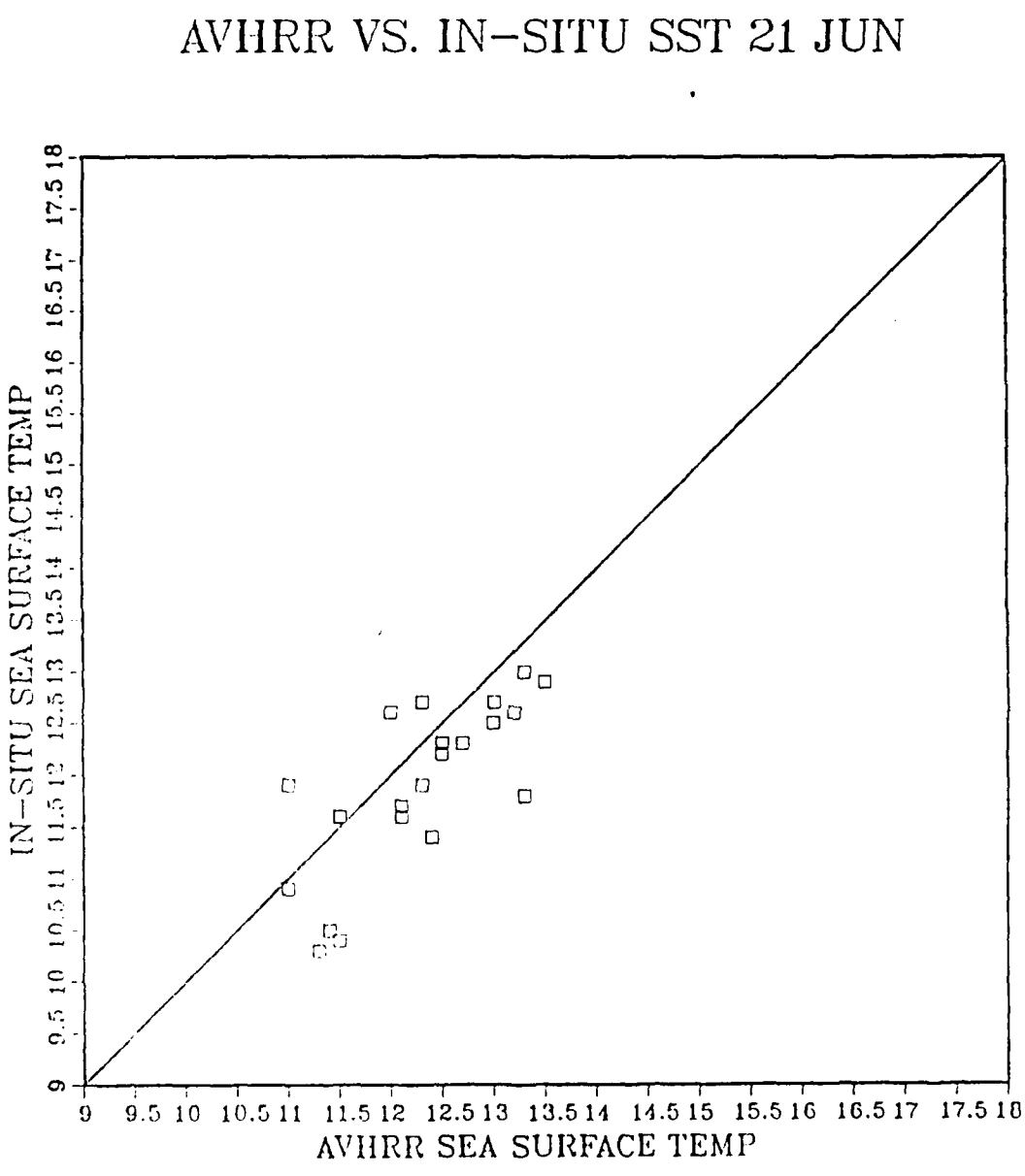

Figure 25 AVHRR versus *In-situ* SST Comparison for June 21, 1987.

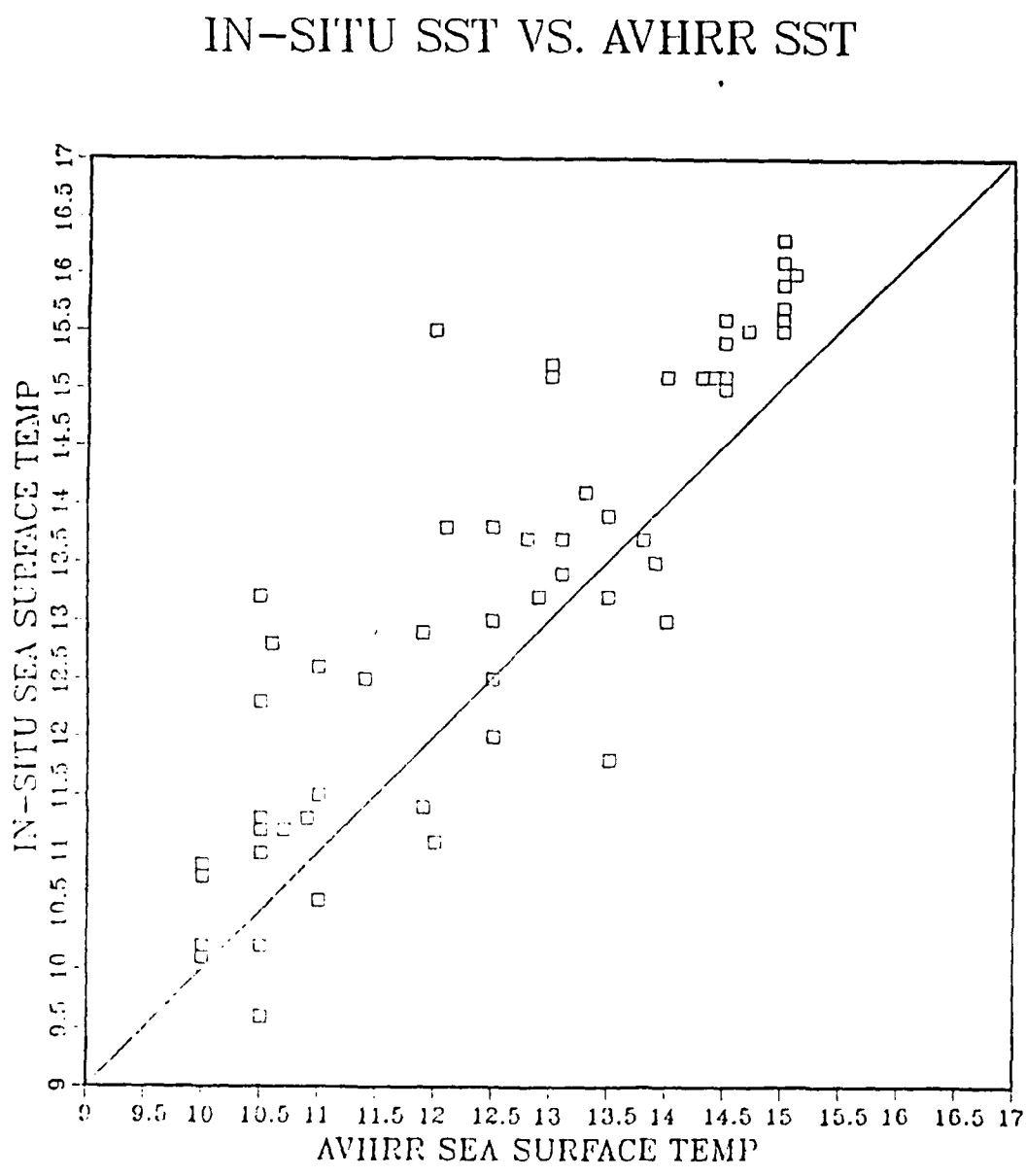

Figure 26 AVHRR versus *In-situ* SST Comparison July 9, 1988.

B. SST REPRESENTATIVENESS OF SUBSURFACE FEATURES

1. CTZE87

a. Phase I (June 16 - 20)

For the first phase of the 1987 cruise the overall area was sampled. This data set yielded its highest correlation at 40 m. The lack of correlation is attributed to the temporal variability between the time the image was taken and the data sampled (6 days). It is felt that the upper 40 m is influenced much more by mixing and heating and can change significantly more over a 6 day period than the deeper waters below 40 m. This would yield lower correlations at the upper levels as seen in (Figure 6). The relatively high correlation value (.78) at 100 m suggests the surface signature is fairly representative to this depth.

Due to the limited area of sampling the number of degrees of freedom used to calculate the 95% level of significance for the correlation coefficient was reduced to four. This yielded a value for the significance level of .88 which was much higher than the statistically significant values for the 1988 data of .70. The second and third phases of the 1987 cruise had an even smaller grid size and made the significance level determination unfeasible.

b. Phase II (June 20 - 22)

In the second phase of the 1987 cruise there were low correlations ranging from .69 at the surface to .74 and 3 m. It is felt that this deviation occurred due to strong surface heating after the image on the 21st of June which raised the *in-situ* SST in the upper few meters in the three days of sampling which followed the image. There were relatively strong correlations down to 50 m suggesting that the filament was not deep in origin but rather more of a surface feature. This was further substantiated in that there were no significant correlations below 50 m.

c. *Phase III (June 25 - 28)*

The third phase of this cruise covered the broad offshore filament extending well offshore. The results obtained were statistically insignificant and show only that the time lag between the data acquisition and the AVHRR imagery (3 days before the beginning of the data sampling) was great enough to yield low correlation levels throughout the water column.

2. CTZE88

a. *Phase I (July 06 - 12)*

The entire data set for this phase of the 1988 cruise yielded significantly correlated data to a depth of 150 m. This suggests that the features had a greater vertical extent than in 1987. The larger grid size also allowed for a greater number of degrees of freedom (8) which yielded a .70 for the 95% level of significance for the correlation coefficient. There were also positive correlations to a depth of 350 m indicating that the surface signature was representative to a greater depth than the previous year.

The filament subset of this phase of the cruise was not statistically significant due to the small size of the data set. Visually the filament appears further north than the *in-situ* data suggests (Figure 5). This is an indication that the filament is actually moving southward with the movement able to be detected in this short time frame (3 days). Comparison of the shape of the correlation profiles between the entire data set and only the filament subset (Figures 15 and 17) suggests that the lower correlations were due to the chosen stations moving quickly out of the filament.

b. *Phase II (July 13 - 18)*

In this phase of the cruise, the correlation was statistically significant (95%) to a depth of 130 m, with positive correlations to 310 m, which was not as deep as the positive 150 m, 350 m values from the previous week.

The filament subset of this phase of the cruise yielded strong positive correlations (.75) down to 150 m. The sharp cutoff between 200 and 250 m suggests that below the 200 m level the warmer water below the filament has been reached and that the filament tilts with depth. This data also indicates that the filament has lost

some of its vertical extent since the correlation coefficient remains positive only to 250 m compared to 360 m in the first week of the cruise.

C. COMPARISON WITH VERTICAL CROSS SECTIONS

The results found by the correlation studies compare very well with the vertical cross sections for this cruise. In the vertical cross section near shore (Figure 27), the upwelling front extends only to about 60 m. Below this depth the temperature contours take on an opposite slope of the surface contours. In the offshore cross sections (Figures 28 and 29), the surface features extend to 500 m.

D. COMPARISON WITH RESULTS OF OTHER STUDIES

1. Simpson et al. (1986)

The results of this study differed from Simpson et al. (1986) in that his correlation function remained positive from the surface to 500 m for the overall area. The only feature which showed any negative correlation was the eddy located approximately 400 nm southwest of Point Conception. The eddy correlation showed a very large drop in correlations between 50 and 70 m and become negative at approximately 80 m. Also, his farfield plot shows relatively strong positive correlations remaining above .60 to 500 m which was much higher than any of the results attained for this study. These differences could be attributed to the location of Simpson's study which was 300 to 400 nm further south than the CTZE studies, and which focused on eddies rather than cold filaments.

It was also unclear in Simpson's paper as to whether the data had been demeaned prior to calculating the correlation coefficient. Based on results he obtained it is felt that these values must have been demeaned. Furthermore, Simpson's paper failed to address significance levels, which appears to be an important aspect of this type of study.

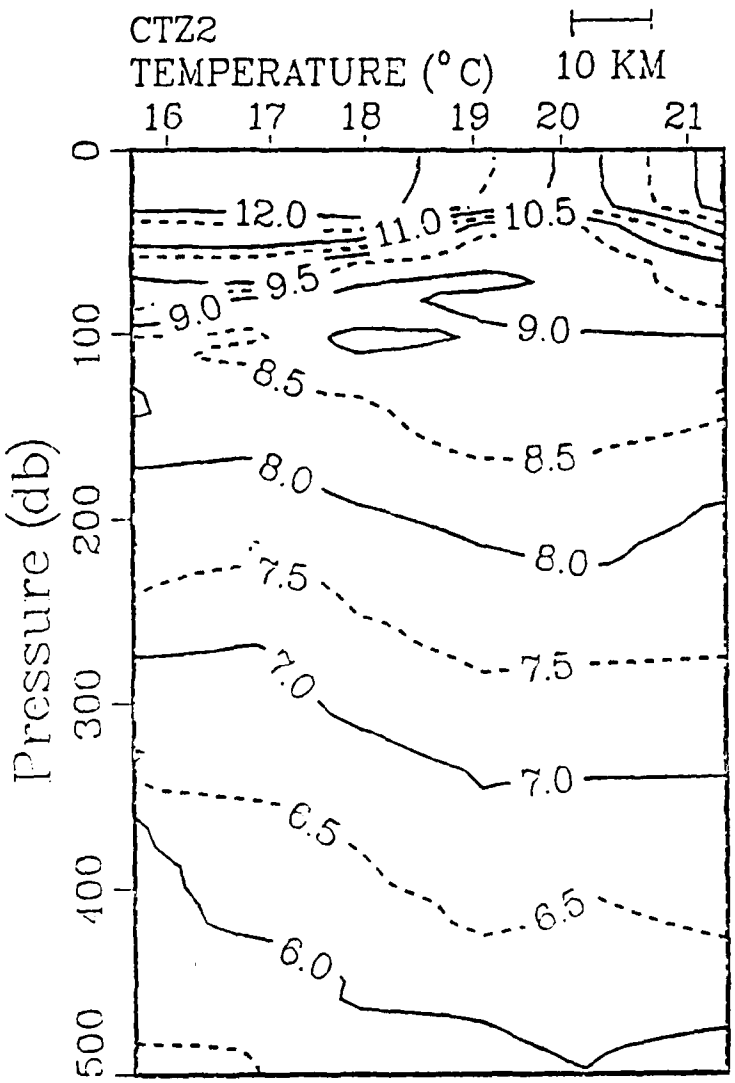

Figure 27 Vertical section of temperature from CTD stations 16 - 21 of Phase I.

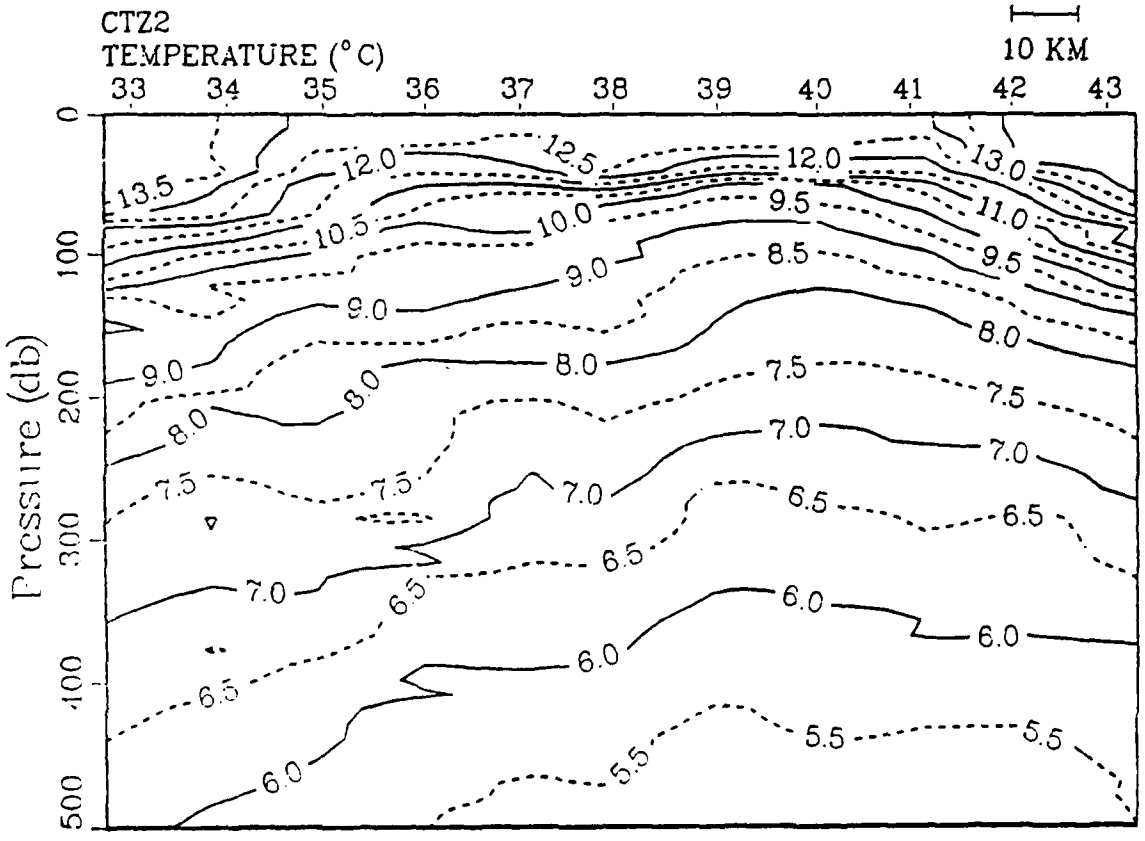

Figure 28 Vertical section of temperature from CTD stations 33 - 43 of Phase I.

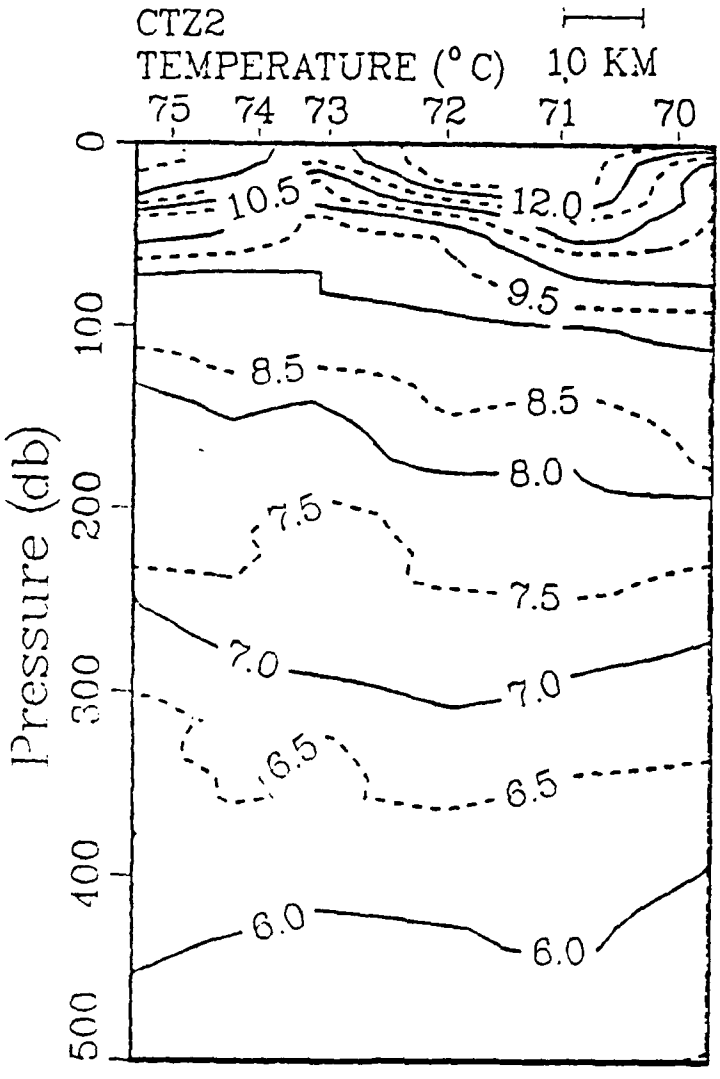

Figure 29 Vertical section of temperature from CTD stations 70 - 75 of Phase II.

2. Rienecker et al. (1987)

The results obtained from the OPTOMA (Ocean Prediction Through Observation, Modeling and Analysis) program (Rienecker et al., 1985) are in fair agreement with the CTZE results. The finding of strong gradients at the southern edge of the filament and weaker gradients to the north is in good agreement (Figures 6, 7, and 12).

The correlation determination was used by Rienecker for the *in-situ* SST field rather than the remotely sensed SST field due to the absence of a "quantitative gridded SST field." Although the features of these two fields show great similarities, it is felt that the two can differ particularly in the station locations near the front. Also it was unclear how the reduced number of degrees of freedom used for the 95% level of significance was obtained. The value of 30 which was used seems unrealistic based on the results of this study. This value for the number of reduced degrees of freedom yielded a 95% level of significance of .37, which based the on present results appears to be much too low, given the size of the OPTOMA study area and correlation scales which are visually evident in the data.

The *in-situ* pattern correlations obtained by Reinecker also were much lower than the results obtained within this study. The surface correlation values are obviously higher based on the *in-situ* SST field being used, but there is a sharp drop down to 0.1 at 80 m and the zero axis is crossed at 120 m.

E. ASW APPLICATIONS

The results obtained in this study could be applied to anti-submarine warfare procedures. By using a satellite image to determine the basic location of the fronts and eddies, one could to a degree determine convergent and divergent areas in the sound velocity determination. One result is that if the time lag is greater than 3 days the correlation between the image and the sub-surface features decreases significantly, limiting the usefulness of the image. However the image could still be used to determine the basic shape and horizontal extent of the various features. The image could also be used to best determine the optimum locations for expendable bathythermograph drops saving both time and money.

V. SUMMARY AND RECOMMENDATIONS

A. SUMMARY

1. CTZE87

The first phase of the 1987 cruise which covered the entire data set area was the only one in which the correlations were significantly correlated. The other two phases which sampled the near shore region and the broad offshore filament did not have enough data points to support a significance correlation calculation. However the strong positive correlations in these phases of the cruise did give an indication of the vertical extent of the near shore features which was approximately 50 m. The broad offshore feature during Phase III had too much time lag between the data sampling and the image (3 days before the start of the sampling) which yielded low correlations. The subsurface maximum occurred due to the temporal offset of the data. This was substantiated by determining the correlation between the *in-situ* SST and temperature field which resulted in a surface maximum.

2. CTZE88

Both phases of the CTZE88 cruise had a larger more uniform sampling scheme which allowed a 95% level of significance to be determined for the correlation coefficient between the SST derived from AVHRR and the in-situ temperature field. The significance level of .70 yielded depths above 150 m which were significantly correlated in the first phase and to 130 m for the second phase of the cruise.

The correlation between the dynamic height (surface relative to 500 db) and the AVHRR derived SST was also significant for both phases of the cruise.

The offshore filament relaxed to the south during this cruise. It also became shallower based on the depth of the zero crossing of the correlation coefficient. The offshore extent (nearly 300 nm) indicates that the filament in the 1988 survey was much stronger than the 1987 filament and that offshore features are deeper than the nearshore ones.

B. RECOMMENDATIONS

It is recommended that the results of this study be compared with different data sets to study changes in the oceanographic features with varying environmental parameters. This could be accomplished by looking at data sets during different parts of the year.

Another area to pursue would be to use the results of this study in conjunction with ASW applications. This would give a user a general idea of the extent of the various features present in their area of interest. Also dynamic height correlations would tell generally where the strong across shore currents were located. Furthermore the user would be able to predict the convergent/divergent areas for sound propagation in the region.

This data set would also be an excellent opportunity to examine feature tracking based on the amount of clear satellite images and extensive oceanographic sampling. The results could be used to determine the surface currents, and compare this with the surface dynamic height and the Acoustic Doppler Current Profiler (ADCP) data.

LIST OF REFERENCES

Beardsley, R.C., Ramp, S.R., and Brown, W.S., "The Nantucket Shoals Flux Experiment 3. The Alongshelf Transport of Volume, Heat, Salt, and Nitrogen.", *Journal of Geophysical Research*, v. 93, No. C11, pp. 14,039 - 14,054, November 1987.

Bernstein, R.L., Breaker, L., and Whritner, R., "California Current Eddy Formation: Ship, Air, and Satellite Results." *Science*, v. 195, pp. 353 - 359, January 28, 1977.

Brink, K.H., and Hartwig, E.O., "Office of Naval Research Coastal Transition Zone Workshop Report." Naval Postgraduate School, Monterey, CA 93943, 67 pp., 1985.

"The Coastal Transition Zone Program", *EOS*, v. 69, No. 27, pp. 698-699, 704, 707, July 5, 1988.

Flament, P., Armi, L., and Washburn, L., "The Evolving Structure of an Upwelling Filament." *Journal of Geophysical Research*, v. 90, No. C6, pp. 11,765 - 11,778, November 1985.

Ikeda, M., and Emery, W.J., "Satellite Observations and Modeling of Meanders in the California Current System off Oregon and Northern California.", *Journal of Physical Oceanography*, v. 14, pp. 1434 - 1450, June 1984.

Jessen, P.F., Ramp, S.R., and Clark, C.A., "Hydrographic Data from the Pilot Study of the Coastal Transition Zone (CTZ) Program 15 - 28 June 1987." *Naval Postgraduate School*, Monterey Ca, 93940, April 1989.

Kelly, K.A., "The Influence of Winds and Topography on the Sea Surface Temperature Patterns Over the Northern California Slope." *Journal of Geophysical Research*, v. 90, No. C6, pp. 11,783 - 11,798, November 1985.

Kosro, P.M., Huyer, J.A., "CTD and Velocity Surveys of Seaward Jets off Northern California, July 1981 and 1982." *Journal of Geophysical Research*, v. 91, pp. 7680 - 7690, June 1986.

McClain, P.C., Pichel, W.G., and Walton, C., "Comparative Performance of AVHRR-Based Multichannel Sea Surface Temperatures." *Journal of Geophysical Research*, v. 90, No. C6, pp. 11,587 - 11,601, November 1985.

Miller, I., and Freund, J.E., *Probability and Statistics for Engineers*, 3d ed., p. 325, Prentice-Hall, Inc., 1985.

Mooers, C.N.K., and Robinson, A.R., "Turbulent Jets and Eddies in the California Current and Inferred Cross-Shore Transports." *Science*, v. 223, pp. 51 - 53, January 6, 1984.

Rienecker, M.M., Mooers, C.N.K., Hagan, D.E., and Robinson, A.R., "A Cool Anomaly Off Northern California: An Investigation Using IR Imagery and In-Situ Data." *Journal of Geophysical Research*, v. 90, No. C3, pp. 4807 - 4818, May 1985.

Rienecker, M.M., Mooers, C.N.K., and Robinson, A., "Dynamical Interpolation and Forecasting of the Evolution of Mesoscale Features Off Northern California." *Journal of Physical Oceanography*, v. 17, No. 8, pp. 1189 - 1213, August 1987.

Simpson, J.J., Koblinsky, C.J., Pelaez, J., Haury, L.R., and Wiesenhahn, D., "Temperature-Plant Pigment-Optical Relations in a Recurrent Offshore Mesoscale Eddy Near Point Conception, California." *Journal of Geophysical Research*, v. 91, No. C11, pp. 12,919 - 12,936, November 1986.

Van Woert, M., "The Subtropical Front: Satellite Observations During FRONTS 80." *Journal of Geophysical Research*, v. 87, No. C12, pp. 9523-9536, November 1982.

Walpole, R.E., and Myers, R.H., *Probability and Statistics for Engineers and Scientists*, 3d ed., p. 347, Macmillan Publishing Company, 1985.

INITIAL DISTRIBUTION LIST

		No. Copies
1.	Defense Technical Information Center Cameron Station Alexandria VA 22304-6145	2
2.	Library, Code 0142 Naval Postgraduate School Monterey, CA 93943	2
3.	Director, Naval Oceanography Division Naval Observatory 34th and Massachusetts Avenue, NW Washington, DC 20390	1
4.	Commander Naval Oceanography Command NSTL Station, MS 39529	1
5.	Commanding Officer Naval Oceanographic Office NSTL Station Bay St. Louis, MS 39522	1
6.	Commanding Officer Fleet Numerical Oceanography Center Monterey, CA 93943	1

7. Commanding Officer 1
Naval Ocean Research and Development Activity
NSTL Station,
Bay St. Louis, MS 39529

8. Commanding Officer 1
Naval Environmental Predicition
Research Facility
Monterey, CA 93943

9. Chairman, Code 68Co 2
Department of Oceanography
Naval Postgraduate School
Monterey, CA 93943

10. Professor S.R. Ramp, Code 68Ra 1
Department of Oceanography
Naval Postgraduate School
Monterey, CA 93943

11. Professor E.B. Thorton, Code 68Th 1
Department of Oceanography
Naval Postgraduate School
Monterey, CA 93943

12. Professor R.L. Haney, Code 63Hy 1
Department of Meteorology
Naval Postgraduate School
Monterey, CA 93943

13. LT Jeffrey S. Best — 2
Naval Eastern Oceanography Center
NAS Norfolk
Norfolk, VA 23460

14. Office of Naval Research — 1
Code 1122CS
800 North Quincy Street
Arlington, VA 22217
ATTN: Dr. Tom Kinder

15. Commanding Officer — 1
Naval Oceanography Command Facility
NAS North Island
San Diego, CA 92111